

Vision Toolkit Part 4. Area of Interest and Associated Algorithms: A Review

Quentin Laborde^{1,2,*}, Axel Roques^{1,3}, Allan Armougom², Nicolas Vayatis¹, Ioannis Bargiotas³, Laurent Oudre¹

¹ Université Paris Saclay, Université Paris Cité, ENS Paris Saclay, CNRS, SSA, INSERM, Centre Borelli, F-91190, Gif-sur-Yvette, France

² SNCF, Technologies Department, Innovation & Research, F-93210, Saint Denis, France

³ Thales AVS France, Training & Simulation, F-95520, Osny, France

⁴ Université Paris-Saclay, Inria, CIAMS, F-91190, Gif-sur-Yvette, France

Correspondence*:

Corresponding Author

quentin.laborde@ens-paris-saclay.fr

2 ABSTRACT

Eye-tracking has become a key methodology for studying human attention, perception, and cognition. A central step in many gaze analysis pipelines consists in transforming raw eye-movement data into sequences of Areas of Interest (AoIs), enabling the use of symbolic and sequence-based models to characterize visual behavior. While this abstraction is essential for quantitative analysis, it also introduces methodological choices that critically shape how gaze dynamics are interpreted. This article reviews major approaches for analyzing AoI sequences, with an emphasis on how gaze dynamics can be modeled, summarized, and compared. We discuss probabilistic and information-theoretic frameworks for characterizing transition structure and uncertainty, as well as pattern-based and sequence-oriented methods designed to reveal recurrent or higher-order viewing strategies. Approaches for extracting representative gaze sequences and for visually exploring AoI dynamics are also examined, highlighting the complementary roles of quantitative modeling and qualitative interpretation. Throughout the review, we emphasize the impact of abstraction choices, particularly AoI definition, on downstream analyses, and discuss key challenges related to scalability, parameter sensitivity, reproducibility, and the analysis of complex or dynamic stimuli. By integrating visualization and modeling perspectives, this work provides a coherent framework for understanding AoI-based gaze analysis and outlines methodological directions for advancing the study of visual behavior.

Keywords: Eye-tracking, areas of interest, gaze dynamics, sequence analysis, visual attention

1 INTRODUCTION

The use of eye-tracking technology has increased dramatically over the past decades, driven by major advances in recording devices that are now more accessible, portable, and capable of delivering high-quality data. Modern eye trackers enable long-duration recordings and support increasingly complex experimental paradigms, both in controlled laboratory environments and in naturalistic settings. While

25 these technological developments have substantially improved the acquisition of raw gaze data, a critical
26 gap remains between the volume of data collected and our ability to interpret the visual strategies and
27 cognitive processes that underlie observed eye movements.

28 Understanding how observers explore visual scenes and how gaze behavior reflects perception,
29 attention, and cognition is of central importance across disciplines such as psychology, neuroscience,
30 human–computer interaction, and ergonomics. However, the growing abundance and complexity of eye-
31 tracking data make intuitive, low-level analysis increasingly impractical. This challenge has motivated
32 the development of *high-level* representations that reduce data complexity while preserving meaningful
33 structure, allowing researchers to efficiently analyze and compare visual strategies at both individual and
34 group levels.

35 Within this context, *areas of interest* (AoIs) have emerged as a key abstraction. Rather than analyzing
36 gaze as a sequence of precise fixation coordinates, AoI-based representations describe gaze behavior in
37 terms of visits to semantically meaningful regions of the visual scene. This abstraction not only simplifies
38 raw gaze data, but also embeds it with contextual information, enabling researchers to reason about *what* is
39 being observed and *how* attention is distributed across relevant visual elements.

40 The use of AoIs is conceptually aligned with principles originating from Gestalt theory Wagemans et al.
41 (2012), which emphasizes that visual perception is structured around coherent wholes rather than isolated
42 sensory elements. From this perspective, individual fixations acquire meaning only when interpreted in
43 relation to larger visual entities. Regardless of the theoretical scope attributed to Gestalt principles, the
44 pursuit of semantic interpretation in eye-tracking data requires that fixations be contextualized within
45 coherent visual regions. AoIs thus provide a natural framework for interpreting scanpaths in terms of the
46 visual elements they traverse, rather than as mere geometric trajectories.

47 AoI sequences can be viewed as a specialized, symbolic representation derived from traditional scanpaths,
48 as introduced in the *Scanpaths and Derived Representations* part of this review series (Laborde et al.,
49 2024c). In this representation, a gaze trajectory is encoded as a sequence of symbols—typically letters or
50 numbers—each corresponding to a specific area of interest, optionally enriched with temporal information
51 such as fixation duration. While this abstraction is conceptually simple, it gives rise to a rich class of
52 analytical methods that differ substantially from those traditionally applied to spatial scanpaths, and that
53 form a distinct and specialized body of literature.

54 More specifically, AoI sequences are constructed by assigning each fixation to the semantic region it falls
55 within, with each AoI associated with a unique symbol. The literature commonly distinguishes between
56 *a priori* AoIs, defined in advance based on stimulus content, and *post hoc* AoIs, inferred directly from
57 gaze data (Huang et al., 2024). In addition, it is often proposed to simplify AoI sequences by collapsing
58 successive fixations within the same AoI, thereby emphasizing transition dynamics between regions rather
59 than fine-grained temporal structure. An overview of this symbolization process is illustrated in Figure 1.

60 This article is the fourth contribution in an ongoing series of methodological reviews dedicated to the
61 analysis of oculomotor signals and gaze trajectories. The first article (Laborde et al., 2024a) synthesized
62 current knowledge on canonical eye movements, with particular emphasis on differences between controlled
63 laboratory conditions and naturalistic viewing. The second article (?) reviewed segmentation algorithms and
64 oculomotor features used to identify and characterize fixations, saccades, and smooth pursuits. The third
65 article (Laborde et al., 2024c) focused on scanpath representations and comparison methods grounded in
66 spatial trajectories. The present work builds on these foundations by concentrating on *AoI-based sequence*

67 representations and on the methods specifically designed to analyze the dynamics, structure, and semantic
68 content of these symbolic gaze sequences.

69 The objective of this review is to introduce and organize the diverse methodologies used to characterize
70 and analyze *high-level* AoI sequence representations. Section 2 briefly reviews approaches for defining
71 areas of interest, which constitute the basis of this representation. Section 3 examines Markov-based models
72 commonly used to describe transitions between AoIs. Sections 4 and 5 address pattern mining techniques
73 and methods for identifying common or representative AoI sequences across observers. Finally, Section 6
74 discusses visualization techniques aimed at facilitating the intuitive exploration and interpretation of AoI
75 sequence dynamics. The principal metrics and algorithms reviewed in Sections 3, 4, and 5 are summarized
76 in Table 1.

77 Before proceeding, two clarifications are necessary. First, although AoI sequences can be treated
78 as symbolic inputs to a variety of sequence analysis methods—many of which were introduced in the
79 *Scanpaths and Derived Representations* review—this article focuses specifically on approaches that analyze
80 AoI sequences in terms of their semantic content and transition structure, rather than their spatial geometry.
81 Consequently, basic AoI-level metrics such as fixation counts or dwell times, which naturally extend the
82 features discussed in earlier parts of this series, are not covered here.

83 Second, our goal is not to provide an exhaustive technical treatment of each approach, but rather to
84 propose a unified conceptual framework that organizes the diversity of existing methods and clarifies
85 their underlying assumptions, required inputs, and interpretability. Throughout this review, we therefore
86 emphasize conceptual relationships between methods and provide references to formal mathematical
87 descriptions and implementation details, enabling interested readers to pursue more technical developments
88 as needed.

2 AOI DEFINITION

89 The analysis of gaze behavior through areas of interest (AoIs) first requires a principled definition and
90 identification of these regions within the visual field. To address this foundational step, a wide range of
91 methods and algorithms have been proposed in the literature. These approaches can be broadly grouped
92 into two complementary families: *stimulus-driven* and *data-driven* methods, also commonly referred to as
93 *a priori* and *post hoc* AoI definitions, respectively.

94 In *stimulus-driven* approaches, areas of interest are defined based on properties intrinsic to the visual
95 stimulus itself. Such properties may include spatial layout, geometric structure, color, contrast, or semantic
96 content that are hypothesized to attract visual attention. These methods typically rely on predefined criteria,
97 often grounded in theoretical or computational models of visual perception, to delineate regions that
98 are expected to be behaviorally or cognitively relevant. By contrast, *data-driven* approaches infer areas
99 of interest directly from experimentally recorded gaze data. In this case, AoIs emerge from the spatial
100 distribution of gaze points and reflect the observer's actual visual exploration behavior. This *post hoc*
101 strategy enables adaptive and empirically grounded AoI definitions, making it particularly well suited
102 to exploratory paradigms, complex scenes, and naturalistic viewing conditions in which relevant visual
103 elements are not known *a priori*.

104 The following sections provide an overview of these two families of methods, outlining their conceptual
105 foundations, typical implementations, and inherent limitations, and highlighting the implications of AoI
106 definition choices for subsequent analyses of gaze behavior.

107 2.1 Stimulus-Driven

108 Historically, areas of interest in eye-tracking studies have most often been defined through manual
109 annotation of the visual stimulus by human analysts. While conceptually simple and intuitive, this approach
110 suffers from several well-documented limitations. Manual annotation is inherently time-consuming,
111 particularly for large datasets or complex stimuli, and often requires the involvement of multiple
112 annotators. This reliance on subjective judgments introduces inter- and intra-annotator variability, which
113 can compromise the robustness, reproducibility, and comparability of AoI-based analyses across studies.

114 Despite these limitations, manual annotation has long remained a prevalent practice in psychological and
115 behavioral research. Its popularity can be attributed to the simplicity of implementation and to experimental
116 traditions that favor controlled and interpretable stimulus manipulations. As a result, user-defined AoIs
117 have been widely employed in diverse application domains, including facial emotion recognition Vassallo
118 and Douglas (2021), the assessment of task-related expertise Wang et al. (2022), and the analysis of eye
119 movement strategies in scientific problem solving Tang et al. (2016).

120 A common strategy in manual AoI annotation consists of overlaying simple geometric shapes — such
121 as rectangles, squares, or polygons — onto the stimulus in order to delineate regions of interest. These
122 shape-based AoIs are favored for their ease of specification and computational simplicity. However, they
123 often fail to align with semantically meaningful objects or perceptual units in the visual scene, which can
124 complicate interpretation and, in some cases, lead to misleading conclusions. Nonetheless, shape-based
125 annotation remains effective in highly structured contexts, such as reading, where discrete visual units
126 — *e.g.* words, lines, or sentences — can be naturally approximated by simple geometric regions Just and
127 Carpenter (1980).

128 To alleviate the subjectivity and scalability issues inherent to manual annotation, a range of automated
129 stimulus-driven approaches has been proposed. One of the earliest such methods consists of partitioning
130 the visual field into a regular grid Mackworth and Morandi (1967), thereby providing a uniform and
131 reproducible segmentation of the stimulus. While straightforward, grid-based approaches ignore the spatial
132 structure and semantic boundaries of visual content, limiting their ability to capture meaningful areas of
133 interest in complex scenes.

134 More refined stimulus-driven approaches aim to define AoIs based on intrinsic properties of the visual
135 stimulus itself, independently of the observer's gaze behavior. Among these, *saliency-based* methods have
136 emerged as a practical compromise between automation and content awareness. These approaches seek
137 to identify visually prominent regions based on low-level image features, such as contrast, orientation,
138 color, or spatial frequency, and are particularly valuable in situations where data-driven AoI definition
139 is impractical—for example, when gaze data are sparse, noisy, or when multiple potential AoIs overlap
140 spatially. Early work by Privitera and Stark (1998, 2000) advocated segmenting images into coherent regions
141 using feature extraction and clustering techniques, laying the foundations for automated, content-aware
142 AoI definition without manual intervention.

143 Several stimulus-driven AoI generation methods are rooted in classical image segmentation techniques Shi
144 and Malik (2000); Arbelaez et al. (2010), which aim to partition an image into perceptually homogeneous
145 regions based on color, texture, or edge information. These methods are particularly effective when clear
146 object boundaries are present in the stimulus, enabling precise delineation of visually meaningful regions.
147 Complementary approaches leverage frequency-domain analyses, such as frequency-tuned salient region
148 detection Achanta et al. (2009) or spatio-temporal saliency estimation Guo et al. (2008). By analyzing

149 the amplitude and phase spectra of images or videos, these techniques highlight regions that stand out
150 perceptually, offering computational approximations of bottom-up attentional mechanisms in human vision.

151 More recently, Fuhl et al. (2018a) proposed an integrated framework for stimulus-driven AoI generation
152 that combines biologically inspired saliency models Itti et al. (1998); Hou and Zhang (2007) with gradient-
153 based image segmentation Fuhl et al. (2015). In this approach, a saliency map is first computed to
154 approximate attentional relevance, and is subsequently segmented to yield precise AoI boundaries adapted
155 to the content of the visual stimulus. While such methods significantly advance the automation and
156 objectivity of AoI definition, they primarily fall within the domain of computer vision. As a result, a
157 comprehensive treatment of these techniques lies beyond the scope of the present review. Broader questions
158 related to the prediction of attention allocation and saliency modeling are discussed in greater detail in the
159 *Scanpaths and Derived Representations* part of this review series Laborde et al. (2024c).

160 The definition of stimulus-driven AoIs becomes particularly challenging in the context of dynamic
161 stimuli. While manual annotation already poses substantial challenges for static images, these difficulties
162 are amplified for videos, interactive environments, or wearable eye-tracking recordings acquired in
163 unconstrained settings. In such cases, the visual content evolves continuously over time, and spatially
164 similar regions may correspond to different semantic entities at different moments. As discussed in the
165 *Neurophysiology and Experimental Paradigms* part of this review series Laborde et al. (2024a), dynamic
166 gaze mapping can be simplified by projecting gaze points onto a fixed reference frame. However, this
167 strategy does not fully resolve the complexities associated with defining temporally consistent AoIs in
168 changing scenes. Recent advances in computer vision have begun to address these challenges through
169 automatic or semi-automatic annotation tools designed for dynamic stimuli Kurzhals et al. (2016); Kopács
170 et al. (2023); Barz et al. (2023). Although these approaches show considerable promise for improving
171 annotation efficiency and consistency, defining reliable and semantically meaningful stimulus-driven AoIs
172 in dynamic environments remains an open and active area of research.

173 2.2 Data-Driven

174 Data-driven approaches define areas of interest directly from experimentally recorded gaze data by
175 exploiting the spatial distribution of fixation points. In contrast to stimulus-driven methods, they do not rely
176 on predefined hypotheses about the structure or semantic organization of the visual stimulus. This makes
177 them particularly well suited to exploratory paradigms, naturalistic stimuli, and situations in which the
178 relevant visual elements are unknown or difficult to annotate *a priori*. A key advantage of data-driven AoI
179 definitions lies in their ability to jointly localize regions of interest and quantify the attentional engagement
180 they elicit, purely from observed gaze behavior.

181 Importantly, data-driven AoIs are not restricted to explicitly fixated visual elements. As emphasized
182 by Boisvert and Bruce (2016), the absence of a direct fixation on a given object — for instance, a
183 face — does not necessarily imply the absence of attentional processing. Peripheral vision, covert
184 attention, and anticipatory gaze behavior may all contribute to visual processing without being reflected in
185 fixation locations alone. By modeling gaze distributions rather than individual fixation targets, data-driven
186 approaches provide a more flexible framework for capturing these broader attentional mechanisms.

187 To account for uncertainty in gaze direction and measurement noise, many data-driven algorithms
188 implicitly tolerate inaccuracies arising from calibration errors, tracker precision limits, or oculomotor
189 overshoots and undershoots. This tolerance distinguishes them from stimulus-driven approaches, which
190 typically assume precise correspondence between fixation locations and visual targets. Readers interested

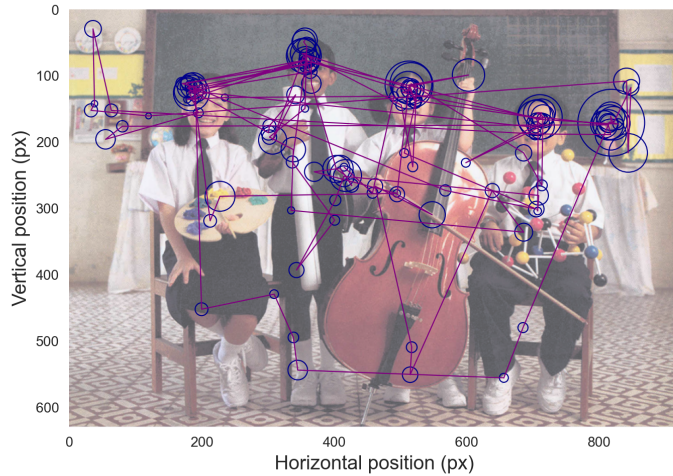


Figure 1a. Input scanpath

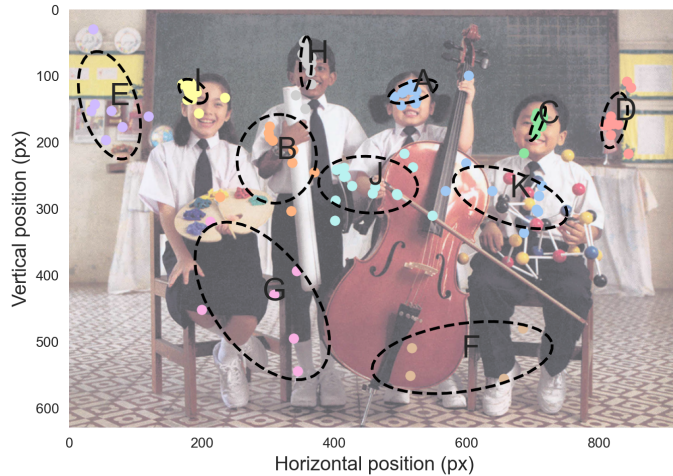


Figure 1b. Areas of interest inferred from *affinity propagation*

Figure 1. Symbolization Process. We illustrate the process of computing areas of interest with a simple example: in Figure 1a, we present a scanpath, which is conventionally used as input for the AoI inference process. Each fixation in the scanpath is utilized to form clusters, here using the *affinity propagation* method. Once formed, these clusters are treated as AoIs. Analyzing the clustering results reveals well-defined AoIs — such as clusters A, C, D, and H — while others appear less relevant, such as clusters F and G.

191 in theoretical discussions of covert attention and inverse inference in gaze modeling are referred to Boisvert
192 and Bruce (2016) and Haji-Abolhassani and Clark (2014).

193 A seminal contribution to the methodological foundations of data-driven AoI generation was provided by
194 Santella and DeCarlo (2004), who outlined three desirable properties for clustering-based AoI algorithms:
195 (i) robustness to initialization, (ii) independence from a predefined number of clusters, and (iii) resilience
196 to outliers. These criteria have since served as reference benchmarks for evaluating the suitability of
197 clustering techniques applied to eye movement data. Most data-driven AoI generation methods rely on
198 standard clustering algorithms, adapted to the specific characteristics of fixation distributions. In this

199 framework, fixations belonging to the same spatial cluster are interpreted as instances of a common area of
200 interest. A schematic illustration of this *symbolization* process is provided in Figure 1.

201 One commonly employed data-driven approach is *k-means* clustering, which is often used either directly
202 (Nguyen et al. (2006); Privitera and Stark (2000)) or in combination with other methods. For instance,
203 Latimer (1988) proposed partitioning gaze data by creating histograms of fixation durations across the
204 visual field, followed by *k*-means clustering of these histograms to identify well-separated and compact
205 fixation clusters. While *k*-means is effective in cases where fixation groups are clearly delineated, its
206 performance deteriorates in more complex scenarios, particularly when the gaze data is noisy. In such cases,
207 the algorithm fails to precisely characterize complex AoIs, and its ability to handle more intricate patterns
208 of visual attention is limited. Additionally, *k*-means clustering requires the user to specify the number of
209 AoIs a priori, which can be problematic in situations where the number of areas of interest is unknown
210 or variable. In practice, this limitation is sometimes mitigated by evaluating several candidate values of *k*
211 using internal validity criteria such as the silhouette score, which quantifies the compactness and separation
212 of the resulting clusters — note that this procedure increases computational cost. The algorithm is also
213 sensitive to outliers, which can distort the results. For these reasons, the use of *k*-means clustering may be
214 constrained, leading researchers to seek alternative approaches that offer greater flexibility and robustness
215 in AoI identification.

216 A more refined alternative to traditional clustering methods is the *mean-shift* approach for defining areas
217 of interest, originally proposed by Fukunaga and Hostetler (1975) and later adapted to eye movement
218 analysis by Santella and DeCarlo (2004). Mean-shift is a non-parametric, density-based technique that
219 operates in two successive stages. In the first stage, known as the *mean-shift procedure*, fixation points
220 are iteratively displaced toward regions of higher local density. Each fixation is shifted according to
221 the weighted mean of its neighbors, where the weights are defined by a kernel function. In practice, a
222 multivariate Gaussian kernel with zero mean and isotropic covariance is commonly employed, with the
223 kernel bandwidth acting as a scale parameter that can be adjusted to reflect the approximate foveal extent
224 of human vision, typically around 5° of visual angle. In the second stage, a distance-based clustering
225 step groups the converged fixation points into distinct clusters, which are subsequently interpreted as
226 areas of interest. A key advantage of the mean-shift approach lies in its robustness to extreme outliers,
227 achieved by limiting the support of the kernel—for example, by assigning zero weight to points located
228 beyond a given multiple of the bandwidth. This mechanism prevents isolated fixations from exerting undue
229 influence on cluster formation. The resulting clusters provide a structured, noise-resistant, and reproducible
230 representation of visual attention patterns (Santella and DeCarlo (2004); Duchowski et al. (2010)). Owing
231 to these properties, mean-shift has become a widely adopted method for AoI generation, particularly in the
232 analysis of noisy or unconstrained eye-tracking data Drusch and Bastien (2012).

233 Another prominent approach for defining areas of interest is the *density-based spatial clustering of*
234 *applications with noise* (DBSCAN) method, originally proposed by Ester et al. (1996). DBSCAN has
235 inspired a wide range of density-based clustering techniques and remains one of the most widely adopted
236 algorithms for data-driven AoI identification, owing to its conceptual simplicity and robustness to noise
237 (McGuire and Chakraborty (2016); Marchal et al. (2016); Reani et al. (2018)). The core principle underlying
238 DBSCAN is that clusters correspond to contiguous regions of high point density, separated by regions of
239 lower density. The algorithm operates using two key parameters: a neighborhood radius and a minimum
240 number of points required to define a dense region. Based on these parameters, DBSCAN introduces
241 the notion of reachability: a fixation is considered directly reachable from another if it lies within the
242 neighborhood radius, and indirectly reachable if it can be connected through a chain of directly reachable

fixations. As a result, fixation points are iteratively classified into three categories: (i) *core points*, which possess a sufficient number of neighbors within the specified radius; (ii) *border points*, which are reachable from core points but do not themselves meet the density criterion; and (iii) *outliers*, which are not reachable from any core point. All fixations that are mutually reachable are grouped into the same cluster, which is subsequently interpreted as an area of interest. By explicitly identifying noise and eliminating the need for an *a priori* specification of the number of clusters, DBSCAN is particularly well suited for gaze data characterized by irregular cluster shapes and variable fixation densities (Ma and Angryk (2017)). A notable extension of DBSCAN is the *ordering points to identify the clustering structure* (OPTICS) algorithm Naqshbandi et al. (2016). Rather than relying on a single density threshold, OPTICS produces an ordering of fixation points based on their reachability distance, enabling the exploration of clustering structures across multiple density levels. This property makes OPTICS especially valuable for eye-tracking datasets in which fixation density varies substantially across regions or observers.

Another density-based approach for defining areas of interest is the *density peak* clustering method, originally introduced by Rodriguez and Laio (2014) and later adapted to AoI identification in eye-tracking studies by Li and Chen (2018). This method relies on the assumption that cluster centers correspond to fixation points characterized by both high local density and a large distance from other fixation points of higher density. More specifically, the algorithm associates each fixation with two quantities: (i) a local density value, typically defined as the number of neighboring fixation points within a user-defined spatial radius, and (ii) a distance measure corresponding to the minimum distance between the fixation and any other fixation exhibiting higher local density. Fixations that simultaneously exhibit high values for both measures are identified as cluster exemplars, which serve as the centers of the resulting areas of interest. To determine the number of AoIs, the algorithm computes the distance–density product for each fixation and sorts these values in descending order. A threshold is then applied to this product, with fixations exceeding the threshold being assigned as AoI centers. The threshold can be empirically defined using either the arithmetic mean or the geometric mean of the distance–density products. The choice of thresholding strategy directly influences the resulting AoI configuration: arithmetic mean thresholds tend to produce fewer, more compact clusters, whereas geometric mean thresholds typically yield a larger number of clusters with increased overlap. While the density peak method offers an intuitive mechanism for automatically determining the number of clusters, its outcomes are sensitive to parameter selection, particularly the choice of neighborhood radius and thresholding strategy. As a result, careful parameter tuning is required to ensure that the resulting AoIs meaningfully reflect the underlying structure of the gaze data.

An alternative family of data-driven approaches for defining areas of interest is based on *exemplar-based* clustering, among which the *affinity propagation* method, originally introduced by Frey and Dueck (2007), has received particular attention in eye-tracking research (Huang et al. (2009); Li et al. (2017)). Unlike variance-minimization or purely density-based techniques, affinity propagation identifies a subset of representative data points, referred to as *exemplars*, which collectively summarize the structure of the dataset. All fixation points associated with the same exemplar are subsequently grouped into a single cluster, interpreted as an area of interest. Affinity propagation operates through an iterative message-passing procedure between all pairs of data points, based on two complementary quantities: *responsibility* and *availability*. Responsibility reflects how well suited a candidate exemplar point j is to represent a given fixation point i , taking into account the relative distances between points and the current availability values. Conversely, availability measures the degree to which a fixation point i is appropriate to act as an exemplar, based on the accumulated evidence provided by other fixation points in the dataset. During the iterative optimization process, responsibility and availability values are updated until convergence. At convergence,

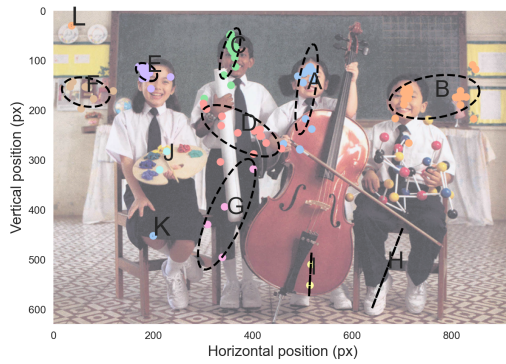


Figure 2a. Areas of interest inferred from *mean-shift*

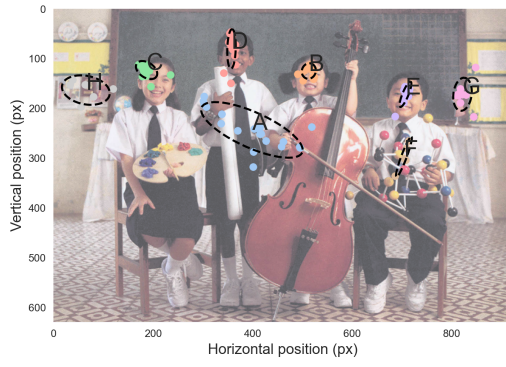


Figure 2b. Areas of interest inferred from *DBSCAN*

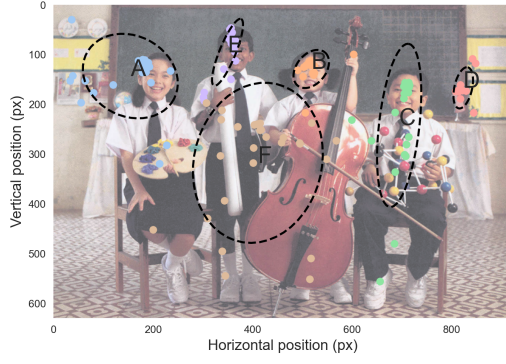


Figure 2c. Areas of interest inferred from *density peak*

Figure 2. Symbolization Process. We illustrate the data-driven AoIs computed using the various algorithms discussed in Section 2.2. A qualitative analysis of the clusters — representing areas of interest — generated by these methods reveals significant variability in results across algorithms. This variability is further amplified by the dependency of many algorithms on one or more parameters, which increases the sensitivity and variability of the outcomes. Therefore, researchers must exercise caution when selecting their approaches and consider adapting their methodology based on the visual context and the specific tasks performed by the viewers.

288 the set of exemplars emerges naturally from the data, eliminating the need for an *a priori* specification of
289 the number of clusters. Fixations are then assigned to the exemplar with which they exhibit the highest
290 affinity, yielding a partition of the dataset into distinct AoIs. Affinity propagation satisfies several key
291 criteria for robust AoI generation outlined by Santella and DeCarlo (2004), notably independence from
292 initialization and from predefined cluster numbers. In addition, the method exhibits a degree of robustness
293 to outliers by forming small auxiliary clusters that isolate atypical fixations, which can be readily identified
294 and excluded from further analysis (Huang et al. (2009); Li et al. (2017)). These properties make affinity
295 propagation a compelling option for AoI identification in gaze datasets characterized by complex spatial
296 structures or heterogeneous fixation distributions.

297 Despite their methodological diversity, a comparative study by Fuhl et al. (2018b) has shown that applying
298 different data-driven AoI generation algorithms to the same gaze dataset can result in markedly different
299 AoI configurations. In particular, approaches based on local maxima thresholding, heatmap gradient
300 analysis, or overlap-based clustering—each grounded in plausible density-driven heuristics—were shown
301 to produce substantially different scene partitions. This observation highlights a fundamental limitation of
302 data-driven AoI definition: the problem is inherently ill-posed, and no single algorithm can be regarded
303 as universally optimal. To illustrate this variability within a unified methodological framework, Figure 2
304 presents AoI configurations obtained using the principal data-driven clustering algorithms detailed in this
305 section. Once defined, these data-driven AoIs constitute the symbolic alphabet from which AoI sequences
306 are constructed, making the properties of the AoI definition stage critical for all subsequent sequence-based
307 analyses.

308 At this point, a few remarks are in order. Firstly, a number of Markov-based methods have been introduced
309 in the literature to define AoIs. These approaches however will be discussed in the Section 3, as they
310 combine the tasks of defining areas of interest and analyzing the attention transition dynamics between
311 these regions. Secondly, by implementing the various methods mentioned above, we can assign the fixation
312 points to distinct areas of interest. Nevertheless, in order to preserve the spatial information of the gaze
313 trajectories, it may be necessary to take into account the locations of the AoIs, and in particular their
314 centers. A first approach, which despite its simplicity remains very popular, simply consists of averaging
315 the coordinates of the different fixations assigned to the same cluster — or AoI. However, such a basic
316 treatment could ignore the spatial relationship among fixations and be sensitive to noise. Alternative
317 approaches have therefore been developed to refine this process. For instance, Pillalamarri et al. (1993)
318 early included several methods to calculate the center of a cluster as the weighted — by duration — mean
319 of clustered fixations and the center of the convex polygon encompassing fixations belonging to the same
320 cluster (Špakov and Miniota (2007)). On the other hand, Wang et al. (2016) proposed to compute a density
321 value — the number of fixations within a given distance threshold — around each fixation of a given cluster
322 and then determine the maximum density value which points to the AoI center. We can also mention the
323 approach suggested by Chen and Chen (2017) who proposed a method based on random walks to identify
324 AoI centers, highlighting the robustness and low susceptibility to outliers of such an approach (?).

325 Finally, we conclude this section by pointing out that, in general, the problem of defining areas of interest
326 has been little explored in the specific case of dynamic stimuli. Indeed, in such a context, spatially identical
327 or close but temporally different fixations may originate from visual elements with totally distinct semantic
328 meanings. Consequently, current data-driven approaches may fail to define precise areas of interest and lead
329 to erroneous conclusions when used as input data for the examination of dynamic eye movements. Recent
330 approaches are beginning to address this issue. We can mention the *AOI bounding boxes estimation* method
331 that uses image segmentation technique to estimate AoI bounding boxes in dynamic stimuli (Lagmay et al.

Method name	Input	Description	Reference
Transition matrix	AoI sequence	Computes transition probabilities between areas of interest as a row-normalized stochastic matrix, from which graph-based metrics — <i>e.g.</i> density, centrality, transitivity, small-worldness and global efficiency — can be derived.	Hsiao et al. (2021)
Transition entropy	Transition matrix	Computes entropy-based metrics characterizing gaze dynamics, including stationary entropy, joint entropy, conditional entropy, and mutual information.	Krejtz et al. (2015)
Hidden Markov model (HMM)	Fixation sequence	Learns a probabilistic generative model of gaze behavior by estimating hidden states and transition probabilities using the Baum–Welch algorithm.	Bilmes et al. (1998)
Fisher vector (HMM-based)	Hidden Markov model	Encodes gaze sequences by computing gradients of the HMM likelihood with respect to model parameters, yielding a fixed-length vector representation.	Kanan et al. (2014)
VHEM clustering	Set of HMMs	Clusters hidden Markov models into groups of similar gaze dynamics and estimates representative HMMs for each cluster using variational inference.	Coviello et al. (2012)
Lempel–Ziv complexity	AoI sequence	Computes the complexity of visual exploration by incrementally identifying novel subsequences while scanning the AoI sequence from left to right.	Lounis et al. (2020)
Common n -gram analysis	AoI sequence	Computes frequency distributions of fixed-length AoI subsequences to capture higher-order transition patterns and local sequential structure.	Ayres et al. (2002)
Sequential pattern mining	Set of AoI sequences	Identifies frequent sequential patterns shared across multiple AoI sequences using data mining algorithms such as Apriori or SPAM.	Ayres et al. (2002)
T -pattern detection	AoI sequence with timestamps	Identifies statistically recurrent temporal patterns in AoI sequences by detecting event structures with consistent inter-event intervals.	Salah et al. (2010)
Longest common subsequence (LCS)	Pair of AoI sequences	Computes the longest subsequence shared by two AoI sequences using dynamic programming, allowing gaps but preserving order.	Bergroth et al. (2000)
Smith–Waterman alignment	Pair of AoI sequences	Performs local sequence alignment using a substitution matrix and gap penalties to identify similar AoI subsequences.	West et al. (2006)
eMINE	Set of AoI sequences	Iteratively derives a consensus AoI sequence by combining global similarity measures and longest common subsequence extraction.	Eraslan et al. (2014)
Scanpath trend analysis (STA)	Set of AoI sequences	Identifies commonly visited and temporally significant AoIs and constructs a representative trend sequence based on fixation frequency and dwell time.	Eraslan et al. (2016)
Candidate-Constrained DTW Barycenter Averaging	Set of AoI sequences	Aggregates multiple AoI sequences into a representative sequence by iteratively minimizing the average dynamic time warping distance.	Li et al. (2017)
Dotplot hierarchical clustering	hierarchical	Extracts common AoI sub-sequences using dotplot analysis and hierarchical clustering based on sequential matching distances.	Goldberg and Helfman (2010)

Table 1. Methods for AoI sequence analysis and their required input representations.

332 (2022)). Conversely, recent publications have proposed leveraging deep learning techniques to identify
 333 AoIs within dynamic visual stimuli (Jayawardena and Jayarathna (2021); Barz et al. (2023); Trajkovska
 334 et al. (2024)). While these approaches appear promising, defining areas of interest in the context of dynamic
 335 stimuli remains a critical research avenue to be further explored in the coming years.

3 MARKOV-BASED MODELS

336 Markov-based analysis provides a probabilistic framework for modeling sequential data by describing
337 system dynamics in terms of state-to-state transition probabilities. A process is said to satisfy the Markov
338 property when the probability of transitioning to a future state depends solely on the current state,
339 independently of the sequence of states that preceded it. While this assumption deliberately abstracts
340 away long-range dependencies, it yields models that are theoretically well grounded, interpretable, and
341 computationally efficient, making them particularly attractive for the analysis of sequential behaviors.

342 In the context of eye-tracking, Markov models are naturally suited to the analysis of gaze dynamics
343 expressed as sequences of areas of interest. Once gaze trajectories have been discretized into AoI sequences,
344 each AoI can be interpreted as a discrete state, and eye movements correspond to probabilistic transitions
345 between these states. Modeling these transitions using Markov-based approaches provides a compact
346 description of visual exploration behavior, capturing systematic patterns in attentional shifts while offering
347 a flexible foundation for both descriptive and inferential analyses.

348 3.1 Transition Matrix

349 Markov-based approaches aim to model transitions between visual elements by estimating transition
350 probabilities, often represented in the form of *transition matrices*. A transition matrix — also referred to as
351 a stochastic or probability matrix — is a square matrix in which each entry corresponds to the probability
352 of transitioning from one current state — *e.g.* an AoI — to another. In an early application of this concept,
353 Ponsoda et al. (1995) developed transition matrices to categorize successive saccade directions. Rather than
354 focusing on AoIs — as is common in modern applications — their matrices represented transitions between
355 eight cardinal saccade directions. Building on this, Bednarik et al. (2005) constructed transition matrices to
356 characterize visual switching behavior across predefined AoIs, providing a framework for analyzing gaze
357 transitions. Fischer and Peinsipp-Byma (2007) further extended the use of transition matrices by combining
358 them with descriptive statistics to compare perceptual responses to the same stimulus. Transition matrices
359 thus offer a powerful tool for summarizing and analyzing gaze patterns, supporting insights into both
360 individual and group-level visual processing behaviors.

361 From a computational standpoint, the elements of a first-order transition matrix are derived from the
362 observed frequencies of transitions between areas of interest. Each matrix entry represents the count
363 of transitions from a specific source AoI to a corresponding destination AoI. To compute empirical
364 probabilities, the matrix is row-normalized, ensuring that the sum of the values in each row equals 1.
365 Consequently, the element in row i and column j reflects the conditional probability of transitioning to the
366 j -th AoI, given that the current fixation is located in the i -th AoI.

367 Although transition matrices offer valuable insights into gaze dynamics, their direct application and
368 analysis remain relatively underexplored in the literature. Nonetheless, several studies have leveraged
369 transition probabilities to infer patterns and dynamics of visual behavior directly (Bednarik et al. (2005);
370 Fischer and Peinsipp-Byma (2007); Vandeberg et al. (2013)). Furthermore, Privitera and Stark (1998)
371 proposed a method for comparing transition matrices by introducing a distance metric designed to quantify
372 similarities or differences in gaze behavior patterns, paving the way for more nuanced analyses of visual
373 attention.

374 Beyond their direct probabilistic interpretation, transition matrices can also be reformulated into
375 alternative representations that emphasize the structural organization of gaze behavior. Another element
376 to consider is the directed graph, which can be directly derived from the transition matrix, as illustrated

377 in Figure 3b. While directed graphs are often introduced primarily as visualization tools, they also
378 constitute a powerful analytical representation of gaze dynamics. In this framework, areas of interest are
379 modeled as nodes, and gaze transitions between them are represented as directed edges whose weights
380 correspond to transition frequencies or probabilities. This graph-based abstraction makes it possible to
381 analyze eye-movement behavior using concepts and metrics drawn from network theory, thereby shifting
382 the interpretation of gaze from a purely sequential process toward a structured visual network.

383 Recent work has demonstrated the relevance of this perspective for characterizing individual differences
384 in visual strategies. For instance, Ma et al. (2023) leveraged graph-theoretic measures computed on gaze
385 transition networks to reveal systematic differences between low-ability and high-ability readers. Their
386 results illustrate how the organization of gaze transitions — rather than isolated fixation metrics — can
387 capture meaningful aspects of cognitive processing during reading.

388 Taken together, graph-theoretic measures provide a compact yet expressive description of gaze dynamics
389 by characterizing both local transition patterns and global network organization. Network *density* reflects
390 the overall richness of visual exploration by quantifying how many transitions between areas of interest are
391 effectively used relative to all possible transitions. Measures of node *centrality* identify areas of interest that
392 play a dominant role in the visual strategy, either by attracting a large proportion of incoming transitions or
393 by acting as frequent intermediaries between other regions. Furthermore *transitivity* captures the tendency
394 of gaze transitions to form locally clustered structures, revealing whether visual exploration favors tightly
395 interconnected subsets of areas, while *small-worldness* describes the coexistence of such local clustering
396 with short paths between distant regions, indicating an efficient balance between focused inspection and
397 broader scene integration. Finally, *global efficiency* summarizes how easily information can propagate
398 across the entire network, providing an aggregate measure of how coherently different areas of interest are
399 connected through gaze behavior.

400 By embedding gaze transitions within a network representation, directed graphs enable the analysis of
401 eye movements at a level that goes beyond pairwise transitions. They allow gaze behavior to be interpreted
402 as an organized system whose structure reflects underlying perceptual, attentional, and cognitive strategies,
403 complementing both transition-matrix-based analyses and more complex probabilistic models introduced
404 in subsequent sections.

405 As previously discussed, a critical characteristic of Markov processes is that the next state — the target
406 AoI — depends solely on the current state, defined as the AoI currently being fixated upon by the observer.
407 This property allows for a mathematically tractable representation of AoI transitions but introduces a
408 significant limitation. Specifically, the assumption that gaze transitions depend only on the current AoI
409 disregards the prior sequence of fixations, effectively ignoring the historical context of gaze behavior.
410 While this simplification may be adequate for straightforward perceptual tasks, it poses challenges for
411 analyzing tasks involving higher-order cognitive processes, where sequential dependencies likely play a
412 critical role.

413 In principle, this limitation can be mitigated by constructing higher-order Markov models that incorporate
414 previously visited AoIs into the transition framework. However, this approach leads to a rapid increase
415 in the number of transition probabilities that must be estimated. Such complexity can make higher-order
416 Markov processes impractical for studying visual dynamics, especially in scenarios where the available
417 gaze data are insufficient to reliably compute all entries in the extended transition matrix (Burmester and
418 Mast (2010); von der Malsburg et al. (2015)).

419 To capture longer-term dependencies in gaze behavior, the *successor representation* (SR) matrix,
420 originally introduced by Dayan (1993), has been adapted for use in the visual domain (Hayes et al.
421 (2011)). The central idea of this approach is to encode not only direct transitions between areas of interest
422 but also the expected sequence of future AoIs inferred from prior observations. In practice, when a
423 transition occurs between AoIs, the SR matrix is updated to associate the originating AoI not only with the
424 immediate target but also with the set of AoIs expected to follow. These associations are weighted by a
425 temporal discount factor, which accounts for the diminishing influence of more distant future states. This
426 approach allows the SR method to provide a richer, temporally extended representation of gaze behavior,
427 accommodating sequential dependencies more effectively.

428 Finally, transition matrices play a pivotal role as foundational components in advanced methodologies,
429 including *hidden Markov models* and *entropy-based analyses*. These approaches leverage the probabilistic
430 structure of transition matrices to model and quantify gaze behavior with greater precision and depth. By
431 capturing the underlying dynamics of visual attention, these methods facilitate a more comprehensive
432 understanding of complex gaze patterns. The intricacies of these advanced applications and their broader
433 implications will be examined in detail in subsequent sections.

434 3.2 Gaze Structure Entropy

435 Entropy, as originally formalized by Shannon (1948), provides a principled measure of uncertainty
436 or unpredictability within a system. When gaze behavior is modeled as a Markov process through an
437 AoI transition matrix, entropy-based measures offer a compact and interpretable way to quantify the
438 structure and complexity of visual exploration. Several entropy metrics have been proposed in this context,
439 each capturing a distinct aspect of gaze organization. Among these, the *stationary entropy* constitutes a
440 foundational descriptor of gaze distribution.

441 Under standard assumptions that the Markov chain is irreducible and aperiodic, it admits a unique
442 stationary distribution, defined as the left eigenvector of the transition probability matrix associated with
443 the eigenvalue one (Meyer (2000)). This stationary distribution characterizes the long-term proportion
444 of time the gaze is expected to spend in each area of interest, independently of the initial fixation state.
445 Applying Shannon entropy to this distribution therefore quantifies the uncertainty associated with gaze
446 position across AoIs (Krejtz et al. (2014)). Low stationary entropy values indicate that visual attention is
447 preferentially concentrated on a limited subset of regions, whereas higher values reflect a more uniform
448 allocation of gaze across the visual scene.

449 While stationary entropy captures the spatial dispersion of gaze over time, it does not account for the
450 dynamics of transitions between areas of interest. To address this limitation, gaze behavior has also been
451 conceptualized as a discrete information channel, referred to as the *gaze information channel* (Hao et al.
452 (2019, 2020)). Within this information-theoretic framework, the *conditional entropy* is defined as the
453 average entropy of the conditional transition probabilities associated with each AoI (Krejtz et al. (2015);
454 Hao et al. (2020)). This metric quantifies the degree of uncertainty in gaze transitions themselves, capturing
455 how predictable or stochastic the shifts of attention are from one region to another. Higher conditional
456 entropy values correspond to more exploratory and less predictable transition patterns, whereas lower
457 values indicate more structured, repetitive, or goal-directed viewing behavior.

458 Beyond stationary and conditional entropy, the gaze information channel framework enables the definition
459 of additional measures that further decompose visual uncertainty and information flow. These include
460 metrics quantifying total uncertainty in gaze behavior, uncertainty conditioned on a specific AoI, as well as
461 mutual information exchanged between pairs of areas of interest or between a given AoI and the rest of the



Figure 3a. Transition matrix

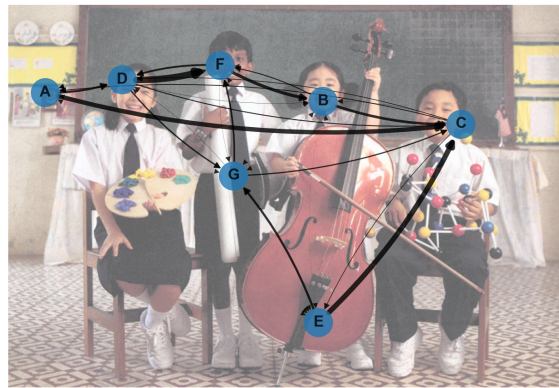


Figure 3b. Directed graph

Figure 3. Inferred Markov model. Modeling gaze dynamics as a Markovian process is demonstrated in Figure 3a, which illustrates the transition matrix encoding the probabilities of shifting from one AoI to another. Additionally, a qualitative analysis of the directed graph associated with this transition matrix, presented in Figure 3b, offers valuable insights. This graph is overlaid on the visual stimulus presented during gaze recording, providing contextual information that enhances the interpretation of the observed transitions.

462 scene. Although a detailed exposition of these quantities lies beyond the scope of the present review, they
 463 provide complementary perspectives on how visual information is distributed and transferred during gaze
 464 exploration. Readers interested in the formal definitions and behavioral interpretations of these measures
 465 are referred to the comprehensive treatment by Hao et al. (2019).

466 When applied to eye-tracking data, entropy-based metrics offer several practical advantages. First, they
 467 yield scalar descriptors of gaze complexity at the individual level, facilitating aggregation across participants
 468 and experimental conditions. Second, they are well suited for inferential statistical analyses, such as group
 469 comparisons, correlation analyses, or regression modeling, enabling systematic investigation of individual
 470 differences in visual behavior. Entropy measures have, for instance, been used to distinguish eye-movement

471 strategies between expert and novice teachers (McIntyre et al. (2017); Kosel et al. (2021)) and to quantify
472 variations in visual search behavior as a function of task complexity or cognitive load (Krejtz et al. (2014)).

473 Taken together, gaze structure entropy metrics provide a theoretically grounded and computationally
474 efficient means of summarizing both the spatial distribution and temporal organization of visual attention.
475 By complementing transition-matrix-based and graph-based analyses, entropy measures contribute to
476 a more comprehensive characterization of gaze dynamics, while naturally motivating the use of more
477 expressive probabilistic models discussed in the following sections.

478 3.3 Hidden Markov Models

479 Recent studies have employed *Hidden markov models* (HMMs) to capture the temporal dynamics of gaze
480 behavior. Like first-order Markov models, HMMs govern the transitions between states through a first-order
481 Markov process. However, the key distinction in HMMs lies in the term *hidden*, which indicates that the
482 states themselves are not directly observable. Instead, they must be inferred from the relationship between
483 the hidden states — representing areas of interest — and the experimentally observed gaze positions (Chuk
484 et al. (2014)).

485 Specifically, the emission densities, which describe the distribution of successive fixations within each
486 AoI, are modeled using two-dimensional Gaussian distributions. The transitions between hidden states
487 are governed by a probability distribution, which is encapsulated in the HMM's transition matrix. The
488 inference process, which aims to estimate the hidden states, is typically performed using the Baum-Welch
489 algorithm, also known as the forward-backward algorithm. This dynamic programming approach is a
490 special case of the expectation-maximization algorithm (Bilmes et al. (1998)). Its purpose is to iteratively
491 adjust the HMM parameters — namely, the state transition matrix, the Gaussian emission parameters, and
492 the initial state distribution — to maximize the likelihood of the model fitting the observed gaze data.

493 HMM-based approaches have been proposed to model the visual attention process (Haji-Abolhassani
494 and Clark (2014)). If early works assumed that the attentional targets could be defined in advance — for
495 instance building on saliency approaches discussed in the *Scanpaths and Derived Representations* part
496 of this review series (Laborde et al. (2024c)) — more recent works emphasize on the fact that during the
497 inference of HMM-based models, the target selection and AoI centers is governed by a statistical process
498 that is trained on natural eye trajectories measured during task execution. Indeed, if the assumption of *a priori*
499 targets may be valid for simple tasks with objective results, it can appear limited in more abstract or
500 complex tasks where defining the potential targets of attention is not straightforward and typically no prior
501 information about the location of the targets is available to the model.

502 In addition, Gaussian distributions - commonly used as emission probabilities - also take into account
503 overshoots and undershoots when directing the gaze at a given target. Consequently, the assumption of
504 accurate targeting is relaxed in the HMM by using observational distributions over visual targets. In other
505 words, this approach dispenses with the need for a preliminary data-driven definition of AoIs, directly
506 integrated into the analysis of visual dynamics. As such, one popular proposed approach begins by using
507 the *k*-means clustering technique Kaufman and Rousseeuw (2009) to locate — as a first approximation
508 — potential targets in an image or scene and then uses the centroids of these clusters to initialize the
509 HMM-based method for decoding eye dynamics and refining visual targets.

510 From this HMM modeling framework, Haji-Abolhassani and Clark (2014, 2013) proposed the
511 computation of task-dependent HMMs, trained with task-specific eye trajectories under the constraint of a
512 shared covariance matrix across all Gaussian emission densities. This approach allows for the creation of

513 HMMs tailored to specific visual tasks. Experimental gaze data can then be probabilistically assigned to a
514 task using a Bayesian inference framework. In this context, the problem is conceptualized as the *inverse*
515 *Yarbus process*, where the likelihood term is determined by the probability of the observed gaze sequence
516 given the task-dependent HMMs previously trained. Similarly, Coutrot et al. (2018) proposed leveraging the
517 HMM representation of gaze dynamics to infer both tasks and stimuli during eye-tracking experiments. In
518 their approach, HMMs are first used to *encapsulate* the dynamics of individual gaze behavior. The resulting
519 HMM parameters — namely the priors, transition matrix coefficients, and the center and covariance matrix
520 coefficients of the Gaussian emissions — are then used as inputs for multiple machine learning-based
521 classifiers. These approaches, however, must be used with care, as small modification of these parameters,
522 can readily result in misclassification (Ellahi (2022)).

523 A significant limitation of the HMM approach is that the number of states must be defined prior to
524 training. This requirement is feasible for images with a predefined number of areas of interest but becomes
525 problematic for more complex or naturalistic stimuli. The *a priori* assumption of a fixed number of states
526 holds primarily for simple visual stimuli, such as synthetic images. To ensure a more data-driven approach,
527 the number of states should not be predetermined but instead optimized based on the recorded eye-tracking
528 data. One possibility is to employ validation and robustness measures to determine the number of clusters,
529 such as using the silhouette score (Elbattah et al. (2023)) during the k -means clustering step that initializes
530 HMM inference or selecting the number of clusters that maximizes the *a posteriori* probability of the
531 training data (Haji-Abolhassani and Clark (2014)).

532 Alternatively, several authors have proposed incorporating the selection of the number of clusters
533 directly into the HMM inference process, thereby eliminating the need for separate initialization steps
534 and enhancing the adaptability of the model. The *variational approach to Bayesian inference* offers a
535 solution for simultaneously estimating model parameters and determining model complexity (McGrory
536 and Titterington (2009)). Specifically, variational inference places prior distributions on the parameters
537 of the emission densities, transition matrix, and initial state distribution, factoring them to compute the
538 maximum *a posteriori* estimate (Bishop (2006)). This method inherently determines the optimal number of
539 hidden states by pruning unnecessary ones, enabling an automatic selection of model complexity, including
540 the determination of the number of AoIs (Chuk et al. (2014, 2017); Coutrot et al. (2018)).

541 On the other hand, the gaze representation offered by HMMs can be made more compact using Fisher
542 vectors, which are a concatenation of normalized HMM parameters into a single vector. For instance,
543 Kanan et al. (2014, 2015) proposed to use Fisher vectors as input features for common classifications
544 algorithms — *e.g.* support vector machine classification algorithm — to infer an observer’s task. To
545 compute Fisher vectors an HMM — for instance with Gaussian emissions — is learned using maximum
546 likelihood estimation. The parameters of the HMM — including transition probabilities and the probability
547 of observing particular AoI fixation given the internal state — will then reflect the sequential information
548 in the data. The idea of a Fisher kernel is to compute how a new sequence of gaze data would change
549 the parameters of the model — *i.e.* the parameter gradients of the generative model when given a novel
550 gaze trajectory as input. Subsequently, two gaze trajectories from the same category will likely change the
551 model in the same way.

552 Finally, a variational approach (Coviello et al. (2014); Chuk et al. (2014)) has been proposed for clustering
553 individuals HMM. The method, referred to as *variational hierarchical expectation maximization* (VHEM)
554 algorithm, clusters HMMs based on the hierarchical EM (HEM) algorithm. This approach allows clustering
555 a given collection of HMMs into groups of HMMs that are similar, in terms of the distributions they
556 represent. Furthermore, it characterizes each group by a *cluster center*, that is, a novel HMM that is

representative for the group. To cope with intractable inference in the E-step, the HEM algorithm is formulated as a variational optimization problem, and efficiently solved for the HMM case by leveraging an appropriate variational approximation.

One of the main advantages of the VHEM approach lies in the fact that, once the clusters have been learned, a gaze trajectory from a new observer can be compared with these models using a Viterbi decoder — *i.e.* classified into the most similar class, considering the estimated log-likelihood score. For each cluster, the VHEM algorithm also produces a representation HMM — cluster center — which summarizes the common AoIs and transitions in the cluster. Interestingly, if this approach does not produce a representative sequence — see Section 5 — it produces a representative dynamical model between gaze data similarly clustered.

4 PATTERN MINING AND CHARACTERIZATION

As discussed in the previous section, the Markov property provides a convenient and interpretable framework for modeling gaze transitions between areas of interest. However, by construction, first-order Markov models remain limited in their ability to capture long-range dependencies and higher-order structures within gaze sequences. This limitation becomes particularly salient in cognitive tasks that involve planning, reasoning, or strategy formation, where visual behavior often unfolds over extended temporal scales.

To address these limitations, a broad family of methods has been developed to identify and characterize recurrent patterns within AoI sequences. Rather than modeling gaze behavior as a sequence of memoryless transitions, these approaches explicitly seek structured motifs, subsequences, or regularities that recur across time or across observers. Such patterns may reflect stable visual strategies, task-specific routines, or shared modes of information extraction that are not readily captured by transition-based models.

Pattern detection techniques span a wide methodological spectrum, ranging from exhaustive searches for all subsequences of a given length to more flexible approaches that allow for temporal gaps, substitutions, or variations in pattern structure. Importantly, these methods originate from the broader field of pattern mining and sequential data analysis and are not specific to eye-tracking data. Their application to AoI sequences therefore represents a methodological transfer, enabling gaze behavior to be analyzed using tools originally developed for domains such as text processing, bioinformatics, or user interaction modeling.

In the context of gaze analysis, pattern mining approaches provide a complementary perspective to probabilistic and graph-based models. By focusing on the identification of meaningful and recurrent subsequences, they offer a direct way to uncover higher-level regularities in visual exploration, facilitating the comparison of gaze strategies across observers, tasks, or experimental conditions. The following sections review the main families of pattern mining methods that have been applied to AoI sequences, along with their underlying assumptions and interpretative implications.

4.1 Lempel–Ziv Complexity

The complexity of visual scanning behavior can be quantified using *Lempel–Ziv complexity* (LZC), a general-purpose measure originally introduced in the context of information theory to characterize the structural richness of symbolic sequences (Lempel and Ziv (1976)). In recent years, this metric has been adapted to the analysis of eye-tracking data by applying it to sequences of transitions between areas of interest, thereby providing a global, model-free descriptor of gaze dynamics (Lounis et al. (2020)). Within

596 the broader landscape of pattern mining approaches, LZC occupies a distinctive position, as it quantifies the
597 overall sequential complexity of gaze behavior without explicitly defining or extracting individual patterns.

598 Algorithmically, Lempel–Ziv complexity can be understood as an incremental parsing procedure applied
599 to a symbolic sequence. The AoI sequence is scanned from left to right, and each time a novel symbol
600 or combination of symbols is encountered — one that cannot be reconstructed from previously observed
601 subsequences — it is added to a dynamically growing codebook. This codebook thus represents the minimal
602 set of distinct subsequences required to encode the original sequence. Rather than identifying predefined
603 motifs, the parsing process implicitly captures the emergence of new structures as the sequence unfolds,
604 making LZC sensitive to both local novelty and global organization.

605 Subsequently, the Lempel–Ziv complexity of a sequence is defined as the size of this codebook, that
606 is, the number of distinct subsequences identified during the parsing process. Sequences characterized
607 by highly regular, repetitive, or stereotyped gaze transitions typically yield small codebooks and low
608 complexity values. In contrast, sequences that exhibit diverse transition structures, frequent novelty, or
609 less predictable ordering lead to larger codebooks and higher complexity scores. When applied to AoI
610 sequences, LZC therefore provides a compact summary of the richness of visual exploration strategies,
611 reflecting how constrained or diversified gaze behavior is over time.

612 One of the main advantages of LZC lies in its simplicity and computational efficiency. Because it does
613 not require an explicit definition of what constitutes a *pattern*, nor does it rely on assumptions about
614 the temporal scale, duration, or semantic relevance of gaze regularities, LZC can be readily applied to
615 a wide range of experimental paradigms. This property makes it particularly attractive for the analysis
616 of naturalistic or unconstrained viewing conditions, where gaze behavior may be highly variable across
617 observers and tasks, and where meaningful patterns may not conform to simple or predefined templates.

618 At the same time, several considerations are important when interpreting LZC values in the context of
619 gaze analysis. First, LZC is inherently sensitive to sequence length, as longer sequences provide more
620 opportunities for novel subsequences to emerge. As a result, comparisons across observers or conditions
621 typically require controlling for sequence length or applying appropriate normalization procedures. Second,
622 LZC depends on the symbolization scheme used to generate AoI sequences, meaning that differences in
623 AoI definition or granularity can directly influence complexity estimates. These dependencies highlight
624 that LZC should be interpreted as a relative rather than absolute measure of gaze complexity, meaningful
625 primarily within a given representational framework.

626 Finally, while LZC effectively captures the presence and degree of sequential structure, it does not
627 explicitly identify which subsequences or motifs contribute to this complexity. Consequently, LZC is best
628 viewed as a global descriptor that complements, rather than replaces, pattern mining methods aimed at
629 extracting and characterizing specific gaze patterns. In the following sections, we review approaches that
630 explicitly enumerate, compare, and summarize recurrent subsequences within AoI sequences, thereby
631 providing a more detailed and interpretable account of visual scanning strategies.

632 4.2 Common n -gram sequences

633 The use of composite probabilities derived from first — or second — order Markov chains has proven to
634 be a valuable approach for modeling visual perception in simple tasks, particularly when areas of interest are
635 not predefined, as discussed in Section 3. Markov models rely on a limited-memory assumption, whereby
636 the probability of transitioning to a given AoI depends solely on the current state. This property makes them
637 well suited for tasks involving relatively straightforward perceptual processes. However, this memoryless

638 assumption may become overly restrictive when tasks require higher-order cognitive functions or complex
639 decision-making. To overcome these limitations, methods such as n -gram transition analysis have been
640 introduced. These approaches enable a more expressive representation of gaze transitions by explicitly
641 capturing higher-order dependencies across successive AoIs, thereby facilitating a richer characterization
642 of visual dynamics in complex tasks.

643 Common n -gram sequences are a foundational concept in natural language processing (NLP), where they
644 have long been used for language modeling and text prediction. They have also found wide application
645 in bioinformatics, particularly for genome and transcriptome assembly, metagenomic sequencing, and
646 error correction of sequence reads, where they are commonly referred to as k -mers (Melsted and Pritchard
647 (2011)). In the context of AoI sequence analysis, an n -gram corresponds to a contiguous subsequence of n
648 successive AoIs. Under this formulation, an n -gram model predicts the occurrence of a given AoI based on
649 the $n - 1$ preceding AoIs, thereby encoding local temporal dependencies that extend beyond first-order
650 transitions.

651 To compute n -gram statistics, combinatorial methods are used to enumerate all possible subsequences
652 of length n defined over a given AoI alphabet. The occurrences of these combinations within the AoI
653 sequence are then counted and normalized by the total number of subsequences, yielding a distribution of
654 n -gram frequencies. This procedure can be applied to simple transitions between two AoIs, referred to
655 as *bi-grams*, or extended to longer n -grams that capture increasingly rich temporal context. In principle,
656 there is no upper bound on the length of n -grams that can be analyzed. In practice, however, the number of
657 unique n -grams grows exponentially with n , leading to increasingly sparse distributions that can undermine
658 interpretability and statistical robustness (Kübler et al. (2017)). Consequently, the use of long n -grams is
659 typically constrained by computational feasibility and diminishing returns in terms of informative content.

660 In the specific context of AoI sequence analysis, n -gram methods have been applied to a variety of
661 cognitive studies to uncover underlying reasoning processes. For instance, Plummer et al. (2017) employed
662 tri-grams of AoI fixations to investigate how individuals reason about rational numbers, comparing fixation
663 sequences to determine whether observers relied on counting-based or comparison-based strategies. This
664 work illustrates how n -gram analysis can be used not only to describe gaze patterns, but also to probe the
665 temporal organization of information processing during reasoning tasks.

666 Beyond task-specific investigations, n -gram analysis has proven valuable in broader contexts aimed at
667 characterizing perceptual efficiency and expertise. For instance, Lounis et al. (2021) examined the frequency
668 of increasing-length n -grams to compare novice and expert pilots, while Wang et al. (2022) used n -gram
669 statistics to quantify cognitive processes and learning progression across trials in an airplane assembly task.
670 These studies demonstrate the utility of n -gram analysis for identifying patterns that differentiate expertise
671 levels or cognitive stages during task performance.

672 Several authors have further investigated the influence of n -gram length on the ability to discriminate
673 between observers or groups. In particular, Reani et al. (2018) reported that subsequences of four or more
674 AoIs were often ineffective at distinguishing between groups in complex reasoning tasks, suggesting
675 that relatively short n -grams may be more informative for capturing meaningful patterns in human gaze
676 behavior. This finding emphasizes the importance of selecting an appropriate n -gram length that balances
677 representational expressiveness with statistical robustness.

678 To compare n -gram frequency distributions across observers or experimental conditions, divergence
679 measures such as the *Hellinger distance* (Hellinger (1909)) have been shown to be particularly effective
680 (Reani et al. (2018)). This distance provides a stable, non-parametric measure of dissimilarity between

681 discrete probability distributions and is less sensitive to zero-probability events than alternatives such as
682 the Kullback–Leibler divergence (Van Erven and Harremos (2014)), making it well suited for the sparse
683 distributions commonly encountered in n -gram analysis.

684 In a broader methodological context, it is worth noting that n -gram analysis constitutes a foundational
685 component of more advanced sequence comparison and characterization approaches. For example, the
686 *Subsmatch* algorithm — described in the *Scanpaths and Derived Representations* part of this review series
687 — relies explicitly on n -gram representations to compare gaze sequences. More generally, n -grams serve as
688 versatile building blocks across a wide range of algorithms in different domains, underscoring their broad
689 applicability and methodological significance.

690 Despite their flexibility and interpretability, n -gram approaches remain limited by their reliance on
691 fixed-length, contiguous subsequences. They do not account for temporal gaps, variability in pattern
692 realization, or hierarchical organization of gaze behavior. As a result, while n -grams provide valuable
693 descriptive insight into local sequential structure, they may fail to capture more complex or temporally
694 flexible patterns of visual exploration. These limitations motivate the use of more expressive pattern mining
695 techniques, which aim to identify recurrent gaze patterns while allowing for temporal variability and
696 structural flexibility. Such approaches are reviewed in the following sections.

697 4.3 Sequential Pattern Mining

698 A distinct approach to analyzing AoI patterns of varying lengths relies on *sequential pattern mining*,
699 a specialized subfield of frequent pattern mining originally developed in the context of market basket
700 analysis (Agrawal et al. (1993)). Unlike classical frequent itemset mining, sequential pattern mining
701 explicitly incorporates temporal ordering constraints, enabling the discovery of patterns that unfold over
702 time (Agrawal and Srikant (1995)). More generally, sequential pattern mining algorithms are applicable
703 whenever the objective is to identify frequent subsequences in datasets composed of temporally ordered
704 elements, making them particularly well suited for the analysis of gaze trajectories expressed as AoI
705 sequences.

706 In eye-movement research, one of the earliest and most widely adopted families of sequential pattern
707 mining methods is based on the *Apriori* principle. Apriori-based sequential mining algorithms aim to
708 discover frequent ordered subsequences by exploiting the anti-monotonicity property of pattern support,
709 which allows infrequent candidates to be pruned early during the search process. These methods provide a
710 natural extension of frequent itemset mining to temporally ordered data and have been extensively used
711 in domains where interpretability and explicit pattern enumeration are desired. In the context of gaze
712 analysis, several *Apriori*-based sequential mining algorithms have been applied to analyze AoI patterns.
713 For instance, such approaches have been used to study how undergraduate computer science students read
714 and comprehend pseudo-code (Obaidellah et al. (2020)).

715 Originally proposed by Agrawal et al. (1994), the Apriori algorithm identifies frequent itemsets through
716 an iterative, level-wise search strategy, in which frequent n -itemsets are used to generate candidate
717 $(n + 1)$ -itemsets. This procedure is guided by the Apriori principle, which states that any superset of an
718 infrequent pattern cannot itself be frequent, thereby substantially reducing the search space. When adapted
719 to sequential data, Apriori-based methods enable the discovery of frequent ordered AoI subsequences.
720 However, despite their conceptual simplicity and interpretability, these algorithms remain computationally
721 demanding due to the need for repeated database scans and the combinatorial growth of candidate patterns.

722 An important improvement over classical Apriori-based approaches is the *Sequential Pattern Mining*
723 (SPAM) algorithm, introduced by Ayres et al. (2002). SPAM adopts a depth-first search strategy combined
724 with a vertical bitmap representation of the data, allowing for efficient support counting and substantial
725 compression of the search space. This representation is particularly advantageous for mining long sequential
726 patterns, as it enables compact storage and fast logical operations. In the context of eye-movement analysis,
727 SPAM has been successfully applied to identify frequent AoI patterns across multiple scanpaths (Hejmady
728 and Narayanan (2012)) and has also been used as a reference method for evaluating newly proposed pattern
729 discovery techniques (Eraslan et al. (2016)).

730 Beyond Apriori-based and SPAM algorithms, other well-established mining techniques have also been
731 employed to characterize AoI sequences. For instance, Geisler et al. (2020) proposed using the *MinHash*
732 algorithm to efficiently assess similarity between AoI sequences. Their approach begins by extracting
733 fixed-length subsequences from AoI sequences using a sliding-window procedure that allows for gaps
734 between elements. The frequencies of these subsequences—conceptually similar to n -grams—are then
735 used to construct frequency dictionaries for each sequence. To compare these dictionaries efficiently, the
736 MinHash algorithm is applied to approximate the Jaccard similarity index between sequences. Although
737 not a pattern mining method in the strict sense, this approach enables scalable and robust comparison of
738 AoI sequences based on shared subsequence structure while maintaining computational efficiency.

739 In a broader methodological context, it is worth noting that sequential pattern mining occupies an
740 intermediate position between simple transition-based analyses and more flexible pattern discovery
741 frameworks. By allowing variable-length subsequences and temporal gaps, these methods overcome
742 some of the limitations inherent to fixed-order Markov models and fixed-length n -gram representations.
743 At the same time, their reliance on frequency thresholds and explicit pattern enumeration preserves
744 interpretability, making them particularly attractive for exploratory analyses of gaze behavior. Moreover,
745 n -gram analysis forms a foundational component of more complex comparison and characterization
746 approaches, such as the *Subsmatch* algorithm—described in the *Scanpaths and Derived Representations*
747 part of this review series—and more generally serves as a versatile building block across a wide range
748 of algorithms in different domains. These characteristics naturally motivate the introduction of more
749 expressive pattern detection techniques, discussed in the following sections, which further relax temporal
750 constraints and aim to capture recurrent visual strategies in a more flexible manner.

751 4.4 T-Pattern Detection

752 *T-pattern* detection was originally developed by Magnusson (2000) to identify temporal and sequential
753 structures in behavioral science, particularly in the context of social interactions. Since its inception, this
754 approach has been applied across diverse fields (Mast and Burmester (2011)) and has been extensively
755 utilized to uncover recurring patterns within viewer gaze dynamics in eye-tracking studies (Mast and
756 Burmester (2011); Burmester and Mast (2010); Drusch and Bastien (2012)). In eye-tracking research, the
757 primary objective of T-pattern analysis is to elucidate the temporal organization of visual behaviors that
758 occur frequently and recurrently, thereby revealing structured attentional routines that are not apparent
759 from fixation statistics alone.

760 As originally defined by Magnusson (2000), a T-pattern is a sequence of events that satisfies two essential
761 criteria: (i) the sequence occurs in the data more frequently than would be expected by chance, and (ii)
762 there exists a consistent temporal relationship between the events. Importantly, T-patterns do not require
763 deterministic timing; that is, the inter-event intervals may vary across occurrences and are treated as
764 stochastic rather than fixed quantities. The detection process therefore focuses on identifying a *critical*

765 *interval*, which defines the characteristic temporal window within which successive events of the pattern
766 are expected to occur and distinguishes meaningful temporal structure from random co-occurrence.

767 The algorithm for T-pattern detection operates under the null hypothesis that the events being analyzed are
768 independent Bernoulli processes with constant probabilities of occurrence per time unit over the observation
769 period. Based on this assumption, the algorithm computes the probability that a second event occurs within
770 a specified time interval following a first event (Qazi et al. (2019)). Through an iterative and hierarchical
771 process, detected T-patterns are progressively combined with additional events or with previously identified
772 T-patterns, enabling the discovery of increasingly complex temporal structures. This procedure continues
773 until no further statistically significant T-patterns can be identified.

774 It is important to note that many of the algorithms discussed in the preceding sections primarily focus on
775 the sequential order of events, often disregarding the temporal intervals that separate them. Moreover, a large
776 class of classical data-mining approaches implicitly assumes constant or discretized time steps between
777 events. By explicitly incorporating temporal constraints, T-pattern detection introduces an additional layer
778 of complexity, both conceptually and computationally. As a result, this approach is particularly well suited
779 for AoI sequences of moderate size, for which variations in inter-event timing can be modeled without
780 incurring prohibitive computational costs.

781 Additionally, the detection of T-patterns is highly sensitive to the choice of the significance level parameter,
782 which directly influences the estimation of critical intervals as well as the number and length of the patterns
783 discovered. A stringent significance threshold typically yields fewer and shorter T-patterns, whereas a more
784 permissive threshold facilitates the detection of longer and more numerous patterns. T-patterns can also be
785 filtered according to various additional criteria, such as minimum pattern length or minimum number of
786 occurrences. Consequently, the results of T-pattern analysis are strongly dependent on parameter settings,
787 which may hinder reproducibility and complicate comparisons across studies if not carefully reported.

788 Finally, it should be mentioned that while Magnusson's original T-pattern detection algorithm is not
789 freely available, a number of subsequent studies have provided detailed descriptions of the underlying
790 computational principles, along with several methodological improvements and extensions (Tavenard et al.
791 (2008); Salah et al. (2010); Arora et al. (2017)). These contributions have clarified the statistical foundations
792 of T-pattern detection, proposed alternative search strategies, and introduced several refinements aimed at
793 improving robustness, computational efficiency, and interpretability. In doing so, they have broadened the
794 applicability of T-pattern analysis beyond its original scope and facilitated its integration into contemporary
795 analyses of gaze behavior and other forms of temporally structured behavioral data. Moreover, by making
796 the core ideas and algorithms more accessible, this body of work has enabled researchers to adapt T-pattern
797 detection to diverse experimental contexts and to combine it more readily with other sequence analysis
798 frameworks.

5 COMMON SUBSEQUENCE IDENTIFICATION AND CLUSTERING

799 As outlined in the previous sections, a wide range of methods have been proposed to identify patterns
800 within observer AoI sequences, either by detecting salient sub-sequences within a single AoI sequence or
801 by extracting recurrent patterns across a set of sequences. In these approaches, the objective is primarily to
802 characterize local or global regularities in gaze behavior without necessarily reducing the data to a single
803 representative trajectory.

804 Conversely, an alternative family of techniques aims to summarize a collection of AoI sequences by
805 identifying a single scanpath that is representative of the entire set, commonly referred to as a *representative*

806 sequence or *consensus sequence*. When AoI sequences are used as abstractions of scanpaths, such consensus
807 representations provide a compact description of the visual strategies shared among a group of observers,
808 facilitating both interpretation and comparison across conditions or populations.

809 In this section, we introduce several algorithms that explicitly combine a common AoI subsequence
810 identification step with clustering mechanisms to organize multiple AoI sequences according to shared
811 visual patterns. By jointly addressing the problems of sequence comparison, grouping, and representation,
812 these methods enable the identification of coherent subgroups of observers and the extraction of
813 representative scanpaths for each group. As such, they constitute a natural continuation of the pattern mining
814 approaches described earlier, while shifting the focus from local pattern discovery to global sequence-level
815 synthesis.

816 5.1 Local Alignment Algorithms

817 Local alignment of sequences is a widely adopted technique, especially in bioinformatics, for uncovering
818 shared patterns within data sequences. In this section, the term *local alignment* is used in a broad sense
819 to refer to methods aimed at identifying common subsequences, independently of their absolute position
820 within the full sequences. The identification of the *longest common subsequence* (LCS) plays a critical
821 role in disciplines that analyze related or derived sequences. The goal of local alignment is distinct from
822 that of global alignment methods, which are comprehensively explored in the *Scanpaths and Derived*
823 *Representations* section of this review series (Laborde et al. (2024c)) in the context of scanpath comparisons.
824 Specifically, local alignment emphasizes identifying highly similar subsequences by aligning only the
825 segments that maximize the similarity score within two larger sequences. This approach enables the
826 detection of analogous sub-patterns, even when their positions vary across the sequences under comparison.
827 As a result, local alignment is particularly advantageous for isolating highly similar areas-of-interest
828 subsequences from AoI sequence representations of scanpaths, facilitating deeper insights into shared
829 patterns of visual exploration without necessitating global sequence alignment.

830 A common approach employed to solve the LCS problem between two string sequences leverages
831 dynamic programming (Bergeron et al. (2000)), a method for addressing optimization problems by breaking
832 them into smaller sub-problems and solving them iteratively in a *bottom-up* manner. Specifically, the
833 algorithm constructs a comparison matrix — or table — where one sequence defines the column indices
834 and the other defines the row indices. Each cell in the matrix represents the LCS at that stage, and the
835 matrix is filled iteratively following this rule: if the AoIs corresponding to the current row and column
836 match, the current cell is assigned a value equal to one plus the diagonal element; otherwise, the cell
837 is assigned the maximum value of the previous row or column. The LCS itself can be reconstructed by
838 backtracking from the matrix's final cell to the origin, following the recorded optimal paths. Meanwhile,
839 the length of the LCS is directly obtained from the value of the last cell in the matrix.

840 Alternatively, the *Smith–Waterman algorithm* (Smith et al. (1981)), a highly regarded local alignment
841 method extensively used in bioinformatics for DNA and protein sequence analysis (Setubal et al. (1997)),
842 has been proposed as a robust approach for identifying similar patterns between pairs of observer
843 AoI sequences (West et al. (2006)). This algorithm is particularly well-suited for analyzing localized
844 correspondences between areas of interest, as it excels in identifying optimally aligned subsequences
845 within larger sequences. Similar to the LCS approach, the Smith–Waterman algorithm utilizes a dynamic
846 programming framework for pairwise sequence comparison; however, it introduces several critical
847 enhancements, foremost of which is the incorporation of a substitution matrix that assigns similarity
848 scores to pairs of AoIs. Matches typically receive positive scores, while mismatches are assigned lower or

negative scores, allowing for a flexible similarity metric. This metric can be adapted to specific applications, for example, by reflecting spatial distances between the geometric centers of AoIs or, in more complex cases, semantic relationships between their contents. Another key feature is the algorithm's ability to handle gaps in alignment through a gap penalty function. This function assigns costs for opening and extending gaps, balancing the trade-off between alignment flexibility and sequence integrity. The parameters of the gap penalty function can be customized to suit specific contexts, enabling the algorithm to manage varying levels of sequence fragmentation or noise effectively.

Locally aligning sequences enables the evaluation of pattern similarity between pairs of AoI sequences, a capability particularly valuable in domains such as clinical reasoning. For example, locally aligned AoI sequences can be used to assess expertise by identifying overlap regions between the AoI sequence of a learner and a reference or optimal sequence (Jraidi et al. (2022)). This approach highlights areas where the learner's focus aligns with the reference, providing insights into their cognitive and visual processing strategies. Beyond pairwise comparisons, some studies have extended local alignment-based analyses to groups of observers in order to detect and classify distinctive visual strategies. For instance, Castner et al. (2020b) proposed a method to distinguish expert and novice dentists in their interpretation of dental radiographs. This approach uses hierarchical clustering based on a distance matrix derived from Smith–Waterman pairwise distances. However, this method does not apply local alignment directly to raw AoI sequences; instead, it analyzes features extracted from observers' scanpath trajectories. This adaptation allows the analysis to focus on high-level features of the visual exploration process, such as fixations and transitions, rather than the raw AoI sequence data, providing a more abstracted but still meaningful representation of visual attention.

A related approach is the *eMINE* algorithm introduced by Eraslan et al. (2014), which explicitly bridges pairwise sequence comparison and multi-sequence synthesis. This method combines both global and local alignment techniques to generate a consensus or abstracted string representation from a set of AoI sequences. The process begins by applying the Levenshtein distance, a global sequence similarity measure, to identify the two most similar sequences within the set (Laborde et al. (2024c)). Next, the LCS technique is applied to these sequences to extract their common subsequence, representing the shared visual attention patterns between them. Once the common subsequence is identified, the two original sequences are replaced by this shared subsequence within the set, and the process repeats iteratively until a single consensus AoI sequence remains. This iterative procedure facilitates hierarchical clustering, uncovering common visual strategies among observers and providing insights into shared patterns of visual attention.

While the *eMINE* algorithm provides valuable insights into overarching visual patterns, it also has certain limitations. Specifically, in scenarios involving numerous observers exhibiting slightly divergent visual dynamics, the intermediate steps of the process may lead to the loss of critical visual elements. The creation of short common subsequences at these stages may fail to capture the subtleties of individual observers' strategies, particularly when dealing with heterogeneous or highly variable AoI data. Although hierarchical clustering in *eMINE* offers the advantage of grouping similar visual strategies, its effectiveness is contingent on the degree of similarity between the sequences being analyzed. For groups of observers with considerable variability, this method may require further refinement or the incorporation of additional metrics to preserve the richness of the original sequences and prevent excessive abstraction during intermediate stages.

5.2 Trend Analysis

As previously discussed, common sequences identified through local alignment-based techniques often suffer from reductionism, resulting in scanpaths that are too short for meaningful analysis or further

892 processing. This limitation arises because such algorithms typically retain only those visual AoIs that are
893 shared across all individual AoI sequences, thereby discarding visual elements that appear in a large subset
894 of observers but not universally. As a consequence, small yet behaviorally meaningful individual deviations
895 are frequently overlooked. To address this limitation, Eraslan et al. (2016) introduced the *scanpath trend*
896 *analysis* (STA) approach, which provides a more inclusive clustering strategy. STA not only identifies
897 visual AoIs visited by all observers but also accounts for AoIs visited by the majority, independently of the
898 order in which they are observed.

899 It is important to note that the term *scanpath* is somewhat misleading in this context. Indeed, the initial
900 step of the STA algorithm consists in transforming each scanpath into a sequence of visual elements,
901 making STA particularly relevant for the analysis of AoI sequences. Accordingly, the algorithm first
902 represents individual inputs as sequences of visual elements, which effectively correspond to AoI sequences
903 augmented with fixation durations associated with each visual region.

904 The STA algorithm operates in two main stages. In the first stage, successive fixations on the same visual
905 element are concatenated, and each visit to a given visual element is defined as a *visual instance*. Each
906 instance is characterized by the identity of the visited visual element and a value reflecting the duration of
907 the visit relative to other instances associated with the same element. The algorithm then analyzes these
908 visual instances to identify *trending* visual elements. If a visual instance is shared across all individual
909 sequences—optionally allowing for a tolerance parameter (Eraslan et al. (2017))—it is considered trending.
910 Visual instances that are not fully shared across all sequences are subsequently evaluated based on the
911 amount of attention they receive, quantified in terms of fixation frequency and associated dwell time.
912 Notably, STA does not rely on predefined thresholds. Instead, these criteria are derived directly from the
913 data: a visual instance is considered trending if (i) its total number of fixations is greater than or equal to
914 the minimum fixation count observed for fully shared instances, and (ii) its dwell time is greater than or
915 equal to the minimum dwell time associated with fully shared visual instances.

916 In the second stage, the STA algorithm constructs a *trending sequence* from the set of identified trending
917 visual instances. To determine the position of each instance within the final sequence, STA assigns a
918 priority value reflecting its relative position within the individual input sequences. These priority values are
919 then aggregated across all observers, and the resulting score is used to determine the ordering of visual
920 elements in the consensus sequence. A visual instance that is not shared by all individual sequences—and
921 whose aggregated priority value falls below the minimum priority of fully shared instances—is excluded
922 from the final trending sequence.

923 Conceptually, STA occupies an intermediate position between strict consensus-sequence extraction and
924 frequency-based pattern mining approaches, offering a compromise between robustness to inter-individual
925 variability and the preservation of an interpretable ordered representation of gaze behavior. Originally
926 developed and evaluated for the analysis of visual behavior on web pages, the STA algorithm has since
927 been applied in a variety of contexts. For instance, it has been used in programming-related tasks to identify
928 common code-reading strategies, with the aim of informing the design of pedagogical interventions and
929 improving program comprehension skills (Ahsan and Obaidellah (2023); Tablatin and Rodrigo (2018)).
930 STA has also been employed to investigate differences in AoI sequences between autistic and neurotypical
931 individuals, providing insights into behavioral and cognitive variations in visual attention patterns (Eraslan
932 et al. (2020)). These diverse applications highlight the versatility of STA as a method for capturing shared
933 visual strategies while accommodating individual variability.

934 5.3 Candidate-Constrained Dynamic Time Warping Barycenter Averaging

935 Recently, Li and colleagues introduced the *candidate-constrained dynamic time warping barycenter*
936 *averaging* (CDBA) method, an advanced algorithm for scanpath aggregation (Li et al. (2017); Li and Chen
937 (2018)). The core idea behind CDBA is to aggregate multiple AoI sequences into a single, representative
938 sequence by computing the barycenter of the experimentally recorded sequences. In this context, the
939 barycenter can be understood as a sequence that is, on average, optimally aligned with all input sequences.
940 More specifically, the algorithm seeks to determine a representative AoI sequence that minimizes the mean
941 dynamic time warping distance to each individual sequence, thereby capturing a consensus sequence that is
942 centrally positioned within the set of observed gaze behaviors. This formulation explicitly integrates both
943 spatial proximity and temporal ordering into the construction of the representative scanpath.

944 The CDBA algorithm builds upon the *dynamic time warping barycenter averaging* (DTWBA) framework
945 originally proposed by Petitjean et al. (2011) and operates through two main iterative steps. In the first step,
946 the algorithm computes the *dynamic time warping* (DTW) distance between each individual AoI sequence
947 and an initially defined reference AoI sequence, which is typically randomly initialized — for a detailed
948 presentation of DTW and its properties, the reader is referred to the *Scanpaths and Derived Representations*
949 part of this review series (Laborde et al. (2024c)). This alignment step establishes an optimal temporal
950 correspondence between each input sequence and the current reference sequence, allowing for non-linear
951 temporal deformations.

952 The second step, referred to as the *update step*, consists in refining the reference AoI sequence based
953 on the alignments obtained in the first step. Each element of the reference sequence is updated using
954 a constrained barycenter computed from the AoIs aligned to that position across all sequences. This
955 constrained barycenter is defined as the AoI that minimizes the average distance to the aligned visual
956 elements while satisfying two key constraints: (i) any two contiguous AoI components in the reference
957 sequence must also appear contiguously in at least one of the individual input sequences, and (ii) the
958 occurrence count of any AoI component in the reference sequence must not exceed its maximum occurrence
959 count across the set of input sequences. These constraints ensure that the resulting consensus sequence
960 remains consistent with the structural ordering and frequency characteristics of the original data.

961 The two steps are iteratively repeated until convergence, that is, until the reference AoI sequence remains
962 unchanged across successive iterations, yielding a final representative AoI sequence. Notably, in their
963 original implementation, Li et al. (2017) performed the DTW alignment at the level of individual fixations
964 rather than directly on AoI centers. In this formulation, DTW is computed between fixation sequences and
965 the reference AoI sequence, and the aggregation process is subsequently expressed at a higher level of
966 abstraction during the update step. Specifically, each component of the reference scanpath is updated with
967 the AoI that minimizes the average distance to all fixations aligned to that position. This hybrid formulation
968 allows the algorithm to retain fine-grained spatial information during alignment while producing a symbolic
969 AoI-based representation as the final output.

970 However, the constant switching between two levels of abstraction — fixations and AoIs — can be
971 somewhat confusing, as it blends both detailed fixation-level information with higher-level AoI-based
972 representations. Moreover, there are two important factors to consider when initializing the iterative
973 refinement process: (i) the length of the initial reference sequence, and (ii) the specific elements that
974 comprise the sequence (Petitjean et al. (2011)). Although these factors have been recognized in the
975 DTW Barycenter Averaging literature, they have not been explicitly addressed by Li et al. (2017) in the
976 context of the CDBA algorithm. Specifically, the length of the starting reference AoI sequence, when the

977 input sequences vary in length, could significantly affect the process of generating a consensus sequence.
978 Inadequate consideration of these factors may lead to suboptimal convergence or misalignment, impacting
979 the accuracy and interpretability of the resulting aggregated scanpath. Compared to frequency-based or
980 alignment-based consensus methods such as STA or eMINE, CDBA explicitly optimizes a geometric
981 notion of centrality under temporal alignment constraints, making it particularly suitable when spatial
982 information and sequence timing are critical.

983 5.4 Dotplot Clustering

984 *Dotplots* are a sequence comparison technique used to measure the similarity between two or more
985 symbol sequences by highlighting common subsequences and shared symbolic patterns. This method
986 provides a graphical representation for sequence comparison, offering an intuitive visualization of matching
987 subsequences. It allows the comparison of sequences of different lengths, naturally accounting for gaps,
988 while preserving the temporal aspect of the AoI sequence. Dot plots have been applied in various fields of
989 string analysis, such as plagiarism detection in literature and informatics (Church and Heflman (1993)),
990 and the study of biological sequences, also known as the diagram method (Gibbs and McIntyre (1970)),
991 the enhanced graphic matrix procedure (Maizel Jr and Lenk (1981)), or dot-matrix plots (Huang and Zhang
992 (2004)).

993 In brief, a dotplot can be considered a discrete variation of a cross recurrence plot — for a detailed
994 discussion, refer to the *Scanpaths and Derived Representations* part of this review series (Laborde et al.
995 (2024c)). The dotplot matrix visualizes the temporal coupling between two AoI sequences, with the vertical
996 axis representing AoIs from the first sequence and the horizontal axis representing AoIs from the second
997 sequence. A dot is placed when fixations from both sequences coincide within the same AoI, and the
998 position is left empty otherwise.

999 Once the dotplot is computed, representative scanning strategies can be derived. These are reflected by
1000 diagonally aligned sequences of dots, representing common sub-sequences or recurring patterns of AoI
1001 sub-sequences across both sequences. Note that, while recent studies have proposed using *cross-recurrence*
1002 *quantification analysis* between AoI centers to quantify visual attention and workload variations (Atweh
1003 et al. (2023)), the dotplot approach leverages the semantic abstraction provided by AoIs more effectively.
1004 It focuses not on the geometric properties of the visualized regions, but on their categorical membership
1005 within the same AoI.

1006 Additionally, in the context of eye movement analysis and AoI pattern assessment, some researchers
1007 have suggested accounting for the differential frequency of AoI occurrences — as some AoIs are more
1008 frequent than others — by weighting each dot (Goldberg and Helfman (2009)). Specifically, a weighting
1009 function introduced by Church and Helfman (1993) assigns to each dot the inverse of the frequency of
1010 that AoI in the concatenated sequence. This allows each dot to be classified as a significant match or not,
1011 based on whether its weight exceeds a predefined frequency threshold. This threshold may be manually set
1012 (Goldberg and Helfman (2010)) or computed experimentally, with significant matches corresponding to
1013 weights greater than one standard deviation from the mean.

1014 Beyond simple qualitative analysis, Goldberg and Helfman (2009) proposed a two-step linear regression
1015 process to extract statistically significant patterns from dot plot pairs derived from a set of AoI sequences.
1016 In the first step, a linear fit is applied to the significant dots. If the coefficient of determination of the fit
1017 falls below a predetermined threshold, it is concluded that there is no common scanning strategy between
1018 the two AoI sequences, and another pair is considered. In a second step, if the regression line is deemed
1019 acceptable, a second linear fit is performed on the points within a small distance from the regression line.

1020 The final common pattern in the two AoI sequences is defined as the sequence of dots closest to this new
1021 fit. The matching distance is quantified as the number of sequentially matching AoIs between the two
1022 sequences. This two-step procedure can be iteratively applied to each pairwise comparison, allowing for
1023 the identification of additional patterns in the input sequences

1024 Subsequently, clustering algorithms, such as hierarchical clustering, have been proposed (Goldberg and
1025 Helfman (2010)) to identify strategies and sets of scanned regions that match progressively larger numbers
1026 of AoI sequences and individuals. To hierarchically cluster multiple AoI sequences, the two most similar
1027 sequences are first selected from the input set based on the dotplot matching distance defined above. These
1028 sequences are then replaced by their common regression sequence. This process is iteratively repeated until
1029 only a single sequence remains, which represents the common, or dominant (Albanesi et al. (2011)), AoI
1030 sequence.

1031 It is important to note that hierarchical clustering can be used in conjunction with other comparative
1032 methods that enable the computation of distances between pairs of AoIs. As such West et al. (2006)
1033 employed hierarchical clustering techniques to directly analyze visual sequences using distance matrices.
1034 These distance matrices were computed using the Levenshtein distance or the Needleman-Wunsch distance
1035 between pairs of visual sequences. A detailed discussion of these distance measures can be found in the
1036 *Scanpath and Derived Representations* part of this review series (Laborde et al. (2024c)). This leads to
1037 several important observations. First, many of the techniques discussed in this work can be combined to
1038 refine our understanding of visual dynamics. Second, certain methods presented in the *Scanpaths Analysis*
1039 section can be adapted for the analysis of AoI sequences. In particular, methods derived from string edit
1040 distances, which take sequences of symbols as input, can be effectively applied in this context

1041 Finally, dotplot-based approaches illustrate how symbolic sequence comparison, statistical filtering, and
1042 hierarchical clustering can be combined to uncover dominant visual strategies, reinforcing the idea that
1043 meaningful consensus scanpaths emerge from the interplay between local pattern alignment and global
1044 sequence organization.

6 VISUALIZATION METHODS

1045 Quantitative methods have gained prominence in recent decades for their systematic approaches to
1046 identifying distinct gaze behaviors across populations or in response to various stimuli. However,
1047 visualization techniques offer a complementary, exploratory, and qualitative framework for analyzing
1048 gaze data. Beyond their descriptive role, such techniques are particularly valuable for examining the
1049 spatio-temporal organization of gaze behavior, revealing complex relationships that may remain difficult to
1050 capture through numerical summaries alone. By providing an intuitive understanding of gaze dynamics,
1051 visualizations facilitate hypothesis generation, interpretation, and communication of results, which can
1052 subsequently be tested or refined using quantitative methods.

1053 While several reviews have addressed general approaches for visualizing eye-tracking data Blascheck
1054 et al. (2014, 2017); Claus et al. (2023), this section specifically focuses on techniques designed to visualize
1055 AoI sequences. These methods emphasize the dynamics of transitions between areas of interest and the
1056 temporal structure of gaze behavior, often building directly on the analytical frameworks introduced in
1057 the previous sections. By visually depicting how gaze progresses across AoIs and how these regions are
1058 interconnected over time, such visualizations provide an interpretable bridge between symbolic sequence
1059 representations and the underlying cognitive and perceptual processes driving visual attention.

1060 6.1 Spatio-Temporal Based

1061 Beyond their illustrative value, spatio-temporal visualizations of AoI sequences are often used in
1062 conjunction with quantitative models of gaze behavior. In particular, they provide an intuitive means
1063 of inspecting, validating, and interpreting temporal structures revealed by transition-based, entropy-based,
1064 or pattern-mining analyses. Among the earliest spatio-temporal visualizations of gaze data, the *time plot*
1065 Itoh et al. (2000); Räihä et al. (2005) represents discrete areas of interest along the vertical axis and time
1066 along the horizontal axis.

1067 Alternatively, *gaze duration sequence diagrams* depict fixation durations within AoIs as continuous
1068 segments along the vertical axis, with horizontal transitions indicating shifts of attention between regions
1069 Raschke et al. (2012). Variants of these approaches appear frequently in the literature under different names,
1070 yet they share a common structure: AoIs are arranged along parallel timelines on one axis, while the other
1071 axis encodes temporal progression Crowe and Narayanan (2000); Holmqvist et al. (2011); Weibel et al.
1072 (2012). Figure 4 provides a representative illustration of these methods. These visualizations can be applied
1073 to individual participants, aggregated groups, or multiple observers displayed in parallel—often using color
1074 coding to differentiate them. However, when many participants are overlaid, the resulting visual clutter can
1075 substantially reduce interpretability.

1076 To enable comparison between observers, the *scarf diagram* provides a simple yet effective method for
1077 spatio-temporal AoI visualization (Burch et al. (2021); Bakardzhiev et al. (2021); Richardson and Dale
1078 (2005); Kurzhals et al. (2017)) — see Figure 5. This technique represents areas of interest along the vertical
1079 axis, with time progressing on the horizontal axis. Each AoI is assigned a distinct color, and individual
1080 time bars are plotted for each observer. These bars are color-coded to indicate the AoI being observed at
1081 any given moment, enabling an intuitive depiction of gaze transitions over time.

1082 Although scarf diagrams were not explicitly designed to visualize recurrent sequences, they facilitate the
1083 comparison of eye movements across multiple participants and support the identification of simple temporal
1084 patterns, such as sustained attention on a specific AoI or simultaneous focus on similar regions across
1085 observers (Claus et al. (2023)). However, their effectiveness decreases when applied to more complex
1086 datasets. In particular, their ability to convey long or intricate gaze patterns is limited when sequences span
1087 extended time periods or involve multiple overlapping transitions. As the number of AoIs increases, scarf
1088 diagrams also become prone to visual clutter, which can substantially reduce interpretability and hinder the
1089 extraction of meaningful insights.

1090 To address these limitations, Yang and Wacharamanotham (2018) extended scarf plots by introducing
1091 Alpscarf, a compact visualization technique designed to facilitate the identification of visual patterns.
1092 Alpscarf incorporates three main extensions: (i) perceptually optimized color palette heuristics, (ii) three
1093 additional visual components — mountains, valleys, and creeks — and (iii) two alternative modes of
1094 scarf width, namely transition-focus and duration-focus. First, the color heuristics (Bianco et al. (2015))
1095 assign each AoI group—implicitly reflecting a predefined AoI hierarchy—a specific color hue, thereby
1096 minimizing perceptual similarity between adjacent groups and improving visual discrimination. Secondly,
1097 Alpscarf introduces three visual components surrounding each scarf. The height of the mountains reflects
1098 AoI visits that follow a user-defined expected order (e.g., sequential paragraph reading resulting in
1099 prominent mountain structures). The depth of the valleys indicates instances of revisits, with frequent
1100 revisits appearing as wider or deeper valleys. Both mountains and valleys leverage the position channel
1101 to encode transition patterns, while the gaps between the scarf and these components—referred to as
1102 creeks—visually emphasize deviations from expected viewing behavior.

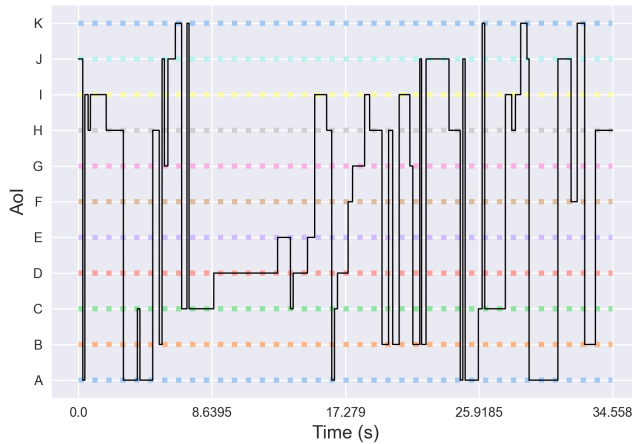


Figure 4. Time plot. A time plot is presented: each colored horizontal line represents an AoI, while the black line traces an individual’s gaze over time — along the horizontal axis — as it transitions from one AoI to another. Despite its simplicity, this method is well-suited for examining the gaze dynamics of a single viewer between AoIs over time.

Finally, Alpscarf offers two modes of scarf width: duration-focus, in which bar width corresponds to the logarithmic fixation duration, and transition-focus, in which all bars are displayed with equal width to emphasize transitions rather than dwell times. More generally, scarf-based representations, and Alpscarf in particular, are frequently used as exploratory complements to sequence analysis methods. They enable researchers to visually assess group-level regularities, temporal alignment, or deviations in gaze behavior, which can subsequently be formalized and quantified using Markov models, entropy-based metrics, or common subsequence analyses.

Another visualization technique closely related to scarf plots is the *gaze stripe* (Kurzhals et al. (2015)). Similar to scarf plots, this method maps time along the horizontal axis and participants along the vertical axis. However, instead of relying solely on color coding, a thumbnail image capturing the local visual context of the stimulus is extracted for each gaze data point and aligned along the timeline. To facilitate the identification of patterns in gaze sequences based on their similarity, Kurzhals et al. (2015) introduced a hierarchical clustering method. In this approach, gaze sequences are represented as leaf nodes, and a cluster hierarchy is constructed using an agglomerative hierarchical clustering algorithm (Hastie et al. (2009)). Similarity between sequences is quantified using a distance metric based on the correlation of hue and saturation histograms derived from the thumbnails. The resulting dendrogram provides a powerful exploratory tool for analyzing sequence similarities and uncovering underlying structural patterns in gaze behavior.

The use of *3D graphics* has also been proposed to simultaneously represent the horizontal and vertical components of the visual field alongside the temporal dimension. However, the introduction of a third dimension requires careful consideration. Perspective effects can complicate the estimation of element sizes, while occlusion caused by overlapping elements may lead to information loss. In the specific context of eye movement analysis, the space-time cube (Kurzhals and Weiskopf (2013)) has been introduced as a promising visualization technique. In this representation, the horizontal and vertical dimensions describe spatial gaze distribution, while time is mapped to the Z-axis. The visual stimulus is displayed at the base of the cube, with gaze trajectories emerging from it and evolving as viewing time progresses. To enhance

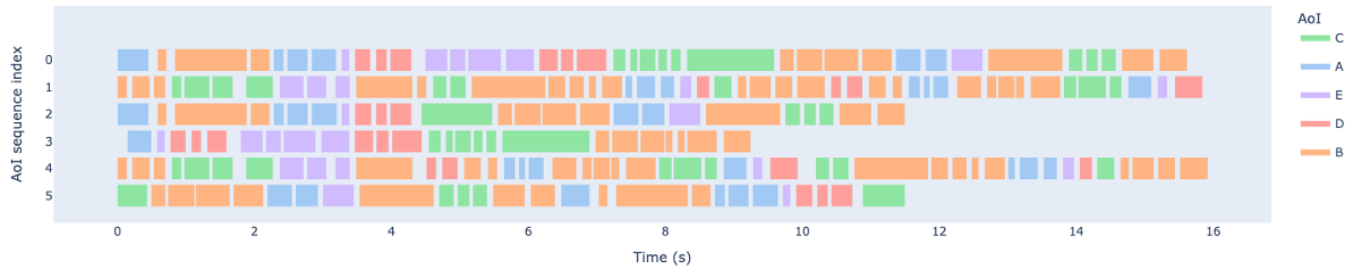


Figure 5. Scarf plot. An illustration of a scarfplot is presented, with six individuals — or six successive recordings from a single individual — displayed along the vertical axis. Time is represented on the horizontal axis, while transitions between AoIs for each individual are shown through changes in color, with each AoI assigned a specific color.

1129 interpretability, segments of gaze traces corresponding to specific areas of interest can be highlighted using
 1130 AoI-consistent color coding. This approach further supports interactivity and dynamism, allowing analysts
 1131 to rotate the cube or animate it along the temporal axis (Kurzhals and Weiskopf (2013)). Despite their
 1132 visual appeal, however, such 3D representations share the main limitations of scarf-based approaches: they
 1133 provide limited support for exploring complex temporal models and become less practical when dealing
 1134 with a large number of input–output relationships.

1135 We conclude this section by introducing *AoI rivers* (Burch et al. (2013)), an interactive visualization
 1136 method designed to explore time-varying fixation frequencies alongside transitions between areas of interest
 1137 in data collected from a large number of participants. This method employs a *Sankey diagram* (Riehmann
 1138 et al. (2005)), which provides an overview of frequently visited AoIs over time while highlighting
 1139 transitions between them. Each AoI is visualized as a color-coded river, with its thickness at any given time
 1140 corresponding to the frequency of visits to that AoI, normalized relative to the maximum AoI frequency
 1141 sum across all time units. The river flows from left to right, dynamically changing width to reflect
 1142 temporal variations in attention. More specifically, transitions between AoIs are depicted as color-coded
 1143 sub-rivers connecting the main AoI rivers, representing transitions between areas over time. Note that
 1144 this representation also accounts for gaze points that are not directly inside an AoI but leave or enter one
 1145 at a later time, which are displayed as *effluents* and *influents*. An example Sankey diagram is provided
 1146 in Figure 6 to illustrate this approach. While AoI rivers provide an effective overview of time-varying
 1147 attention frequencies, they are less suited for revealing hierarchical or long-range sequential structures in
 1148 gaze behavior. As noted by Burch and colleagues (Burch et al. (2013)), these representations are most
 1149 effective when applied to datasets with a limited number of areas of interest. Consequently, AoI rivers
 1150 are best viewed as a complementary tool that emphasizes aggregate temporal trends rather than detailed
 1151 sequential dependencies, motivating the use of transition- and pattern-based visualizations introduced in
 1152 the following subsection.

1153 More generally, spatio-temporal AoI visualizations serve as a conceptual bridge between raw gaze
 1154 recordings and abstract sequence-based representations. By explicitly encoding both the temporal evolution
 1155 of attention and the transitions between areas of interest, these visualizations provide an interpretable
 1156 intermediate layer that facilitates hypothesis generation and exploratory analysis. In practice, they enable
 1157 researchers to visually inspect recurrent patterns, temporal alignments, or deviations across observers,
 1158 which can subsequently be formalized and quantified using the computational models introduced in the

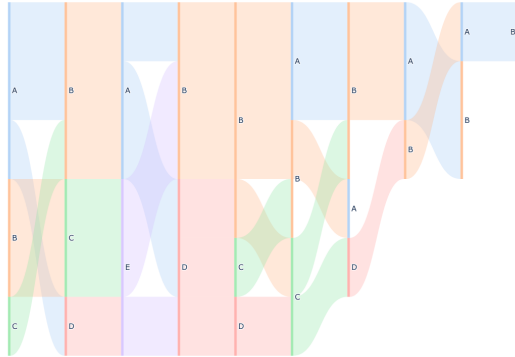


Figure 6. Sankey diagram. An illustration of a Sankey diagram is provided, where each AoI is represented by a distinct color-coded stream. The width of each stream reflects the frequency of visits to the corresponding AoI at any given time, with thicker sections indicating greater attention. The streams flow from left to right, dynamically adjusting in width to depict temporal variations in attention distribution. Transitions between AoIs are represented by interconnecting, color-coded sub-streams that bridge the primary streams, effectively visualizing the movement of attention between different areas over time.

preceding sections. As such, spatio-temporal visualizations play a critical role in validating, contextualizing, and complementing quantitative analyses, ensuring that higher-level sequence models remain grounded in the underlying gaze dynamics.

6.2 Transition Based

Visualizing the transitions of an observer, or, where applicable, a group of observers, presents a significant challenge due to issues such as visual clutter and the loss of explicit temporal information, which may obscure the underlying visual strategies employed by the observer. As a result, various visualization techniques have been proposed to improve the representation and interpretation of transitions between areas of interest (AoIs).

One of the simplest approaches consists in visualizing a previously computed AoI transition matrix (Goldberg and Kotval (1999); Krejtz et al. (2013)), as described in Section 3.1. In a transition matrix, AoIs are ordered along the horizontal axis — rows — and the vertical axis — columns — and each cell contains the count or proportion of transitions between the corresponding AoIs. A color scale is commonly applied to encode the frequency or intensity of gaze transitions, yielding a compact visual summary of pairwise transition probabilities — as illustrated in Figure 3a. This representation provides a direct visual counterpart to a Markov-based transition model and retains all pairwise transition statistics. However, despite this quantitative completeness, transition matrices remain limited from a perceptual and exploratory standpoint. In particular, they do not explicitly convey temporal ordering or higher-order sequential structure, and are often considered less expressive than graph-based visualizations, such as directed graphs, which offer a more intuitive depiction of gaze dynamics between AoIs.

A *directed graph* is a visualization that depicts transitions between areas of interest, with each node representing an AoI and each directed edge illustrating a transition between two AoIs. Although these diagrams are most commonly used to represent the eye movement dynamics of a single participant, they can also be constructed from aggregated or averaged data across multiple observers. In addition, nodes can be resized or color-coded to encode auxiliary metrics, such as fixation duration or visit frequency, while the thickness of the directed edges typically reflects the frequency or probability of transitions between the

1185 corresponding AoIs. While many visualization techniques present the graph independently of the stimulus
1186 (Itoh et al. (1998); Fitts et al. (2005); Tory et al. (2005)), *in-context* directed graphs embed the graph
1187 directly within the visual stimulus (Holmqvist et al. (2003); Hooge and Camps (2013); Opach et al. (2014))
1188 — as illustrated in Figure 3b. This integration enhances interpretability by enabling a direct correspondence
1189 between AoI transitions and stimulus content (Blascheck et al. (2017)), thereby facilitating a more intuitive
1190 understanding of gaze behavior.

1191 However, directed graphs also exhibit several inherent limitations. By construction, they are restricted to
1192 the representation of sequential pairs of fixations, *i.e.* first-order transitions between AoIs, which limits
1193 their ability to convey longer and more complex gaze patterns. Moreover, as the number of areas of
1194 interest increases, directed graphs tend to suffer from visual clutter, making large-scale transition structures
1195 increasingly difficult to interpret. Although a variety of graph visualization techniques have been proposed
1196 to mitigate these issues (Von Landesberger et al. (2011)), scalability remains a central challenge, motivating
1197 the development of alternative transition-based visualizations that better capture higher-order structure and
1198 global gaze dynamics.

1199 An interesting alternative to directed graphs is the use of *chord diagrams*, a class of visualization
1200 techniques designed to represent pairwise relationships between nodes in a compact and symmetric manner.
1201 Their simplicity and intuitive radial layout — in which all nodes can be directly connected to one another
1202 — has led to their widespread adoption in affiliation and relational visualizations Rees et al. (2020). In the
1203 context of gaze analysis, chord diagrams have recently been proposed as effective tools for highlighting the
1204 global structure of eye movement transitions (Connor et al. (2020); Castner et al. (2020a); Wang (2021);
1205 Claus et al. (2023)). In a typical chord diagram, each AoI is represented as a segment along the outer
1206 circumference of a circular layout. Arcs, or chords, are drawn between AoIs, with the width of each arc
1207 proportional to the frequency of transitions between the corresponding visual elements. By construction,
1208 these arcs are symmetrical and therefore do not encode directionality, instead capturing the overall strength
1209 of association between pairs of areas of interest (Blascheck et al. (2013)).

1210 To provide more specific information about gaze dynamics, color-coding schemes can be incorporated
1211 (Connor et al. (2020)) to encode the direction of transitions, for instance by indicating the AoI from
1212 which a transition originates. While this refinement enhances interpretability, it may also increase visual
1213 clutter, potentially reducing the clarity of the visualization when many AoIs or transitions are present. An
1214 illustration of this approach is shown in Figure 7. Although chord diagrams are most often used to visualize
1215 the gaze dynamics of individual observers, they have also been employed for group-level comparisons. For
1216 example, Connor et al. (2020) designed chord diagrams in which arc widths represented differences in
1217 transition frequencies between populations with varying levels of expertise, thereby emphasizing contrasts
1218 in visual strategies. Taken together, matrix-, graph-, and chord-based representations offer complementary
1219 perspectives on gaze transitions, trading temporal specificity and directionality for structural readability
1220 and global relational insight.

1221 To refine transition visualization, Blascheck et al. (2016) proposed to introduce *hierarchical structure*
1222 between AoIs. Specifically, they distinguish between two types of hierarchy: (*i*) a *spatial* hierarchy with
1223 stimuli presenting nested AoIs, and (*ii*) a *semantic* hierarchy between AoIs. Once a hierarchy is established
1224 between areas of interest, Blascheck and colleagues proposed two complementary visual refinements:
1225 a hierarchical transition matrix and a graph-based representation grounded in an AoI tree structure.
1226 The proposed transition matrix visualization enhances a standard transition matrix by incorporating a
1227 hierarchical structure for the Areas of Interest, with the hierarchy displayed as a dendrogram positioned
1228 along the top and left sides of the matrix. Each AoI is represented both in the rows and columns of the

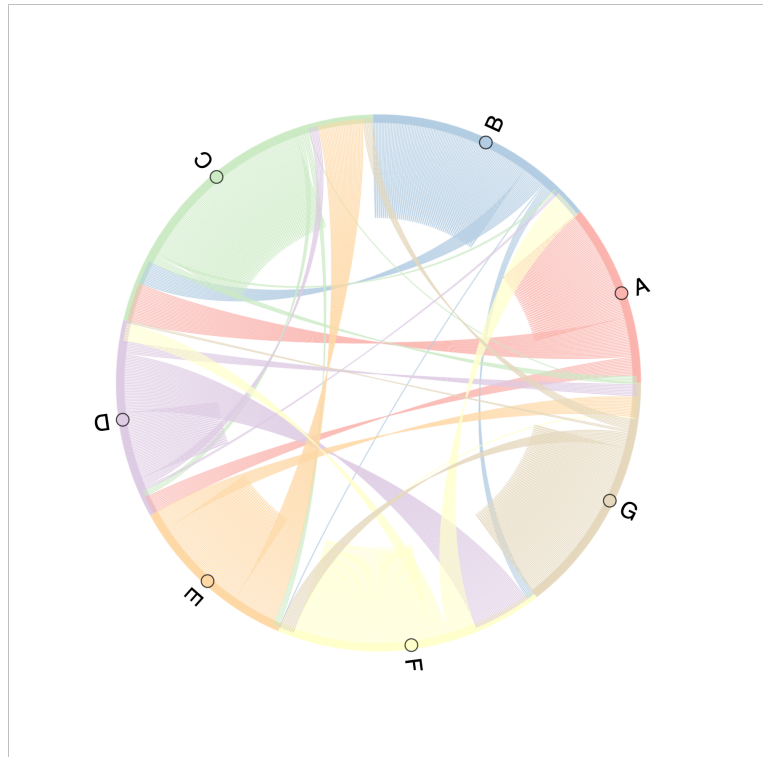


Figure 7. Chord diagram. An illustration of a chord diagram is presented, where each AoI is represented as a segment along the circumference of a circular layout. Arcs, or chords, link the AoIs, with the width of each arc proportional to the frequency of transitions between the respective visual elements. A color-coding scheme is employed to denote the direction of transitions, with arcs taking on the color of their source AoI.

matrix, and a color-coding scheme is applied to reflect the relative importance of transitions associated with each AoI. Specifically, the color of the row headers indicates the total number of outgoing transitions from a given AoI, while the color of the column headers represents the total number of incoming transitions to that AoI.

In addition to the matrix visualization, the AoI hierarchy can be further explored using an AoI tree representation. This tree structure utilizes indented pixel tree plots Burch et al. (2010), where each hierarchical element is represented by a rectangle, and the indentation of these rectangles corresponds to their hierarchical level. The root class and intermediate hierarchical classes are visually distinguished by vertically expanded rectangles, while the leaf nodes, which correspond to individual AoIs, are represented by smaller squares. Subsequently, transitions between AoIs are visualized in a manner similar to directed graphs, with arcs connecting the leaf nodes corresponding to individual AoIs. The width of each arc encodes the frequency of transitions, providing an intuitive visual cue for the intensity of gaze activity between regions.

The methods discussed thus far primarily focus on analyzing sequential pairs of fixations, *i.e.* transitions between two areas of interest. While informative, such pairwise representations provide only a limited view of gaze behavior, as they fail to capture the broader temporal organization and global structure of eye movement sequences. To overcome this limitation and represent the overall dynamics of gaze transitions, the *hierarchical flow of eye movements* approach introduced by Burch et al. (2018) proposes an innovative graph-based visualization.

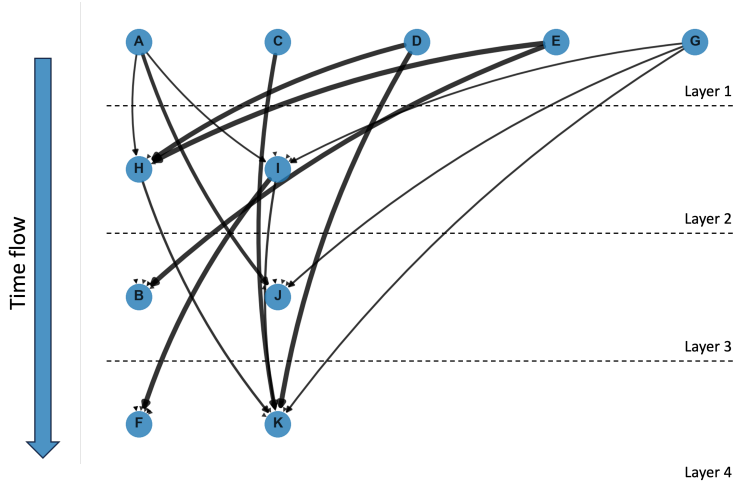


Figure 8. Flow diagram. An illustration of a flow diagram is provided, where AoIs are depicted as circular nodes arranged in vertically stacked layers according to the average order of their appearance in the analyzed sequences. Nodes corresponding to AoIs with earlier occurrences are positioned higher in the diagram, establishing a top-to-bottom flow. Transitions between AoIs are visualized as directed edges, with the thickness of each edge proportional to the frequency of the transitions, effectively highlighting the flow and magnitude of attention shifts.

1248 In this approach, areas of interest are represented as vertices in a graph and visually depicted as circular
 1249 boxes, as illustrated in Figure 8. These vertices are organized into vertically stacked layers according to
 1250 the average order in which they appear within the analyzed AoI sequences. The resulting top-to-bottom
 1251 layout reflects the typical progression of visual attention, with AoIs associated with earlier occurrences
 1252 positioned higher in the diagram. Similar to directed graphs, transitions between AoIs are represented
 1253 by oriented edges, whose thickness encodes transition frequency. The visualization thus builds upon a
 1254 previously computed AoI transition matrix to highlight dominant transition patterns. Unlike standard
 1255 directed graphs, however, the layered structure explicitly embeds temporal ordering into the spatial layout,
 1256 allowing dominant gaze flows and global viewing strategies to be interpreted at a glance.

1257 To highlight visual patterns at the sequence level, a *word tree* (Wattenberg and Viégas (2008)) visualization
 1258 can be employed to compare AoI sequences across multiple observers. Tree structures are particularly well
 1259 suited for illustrating the sequential organization of gaze patterns. In a word tree, each node represents an
 1260 AoI, and branches display subsequent AoIs or subsequences of AoIs—many branches indicating a diversity
 1261 of search strategies—thereby mapping the flow of gaze behavior. Each path from the root to a leaf node
 1262 represents a unique observed AoI sequence, and, with the exception of the root, each node is connected to
 1263 its parent by a curved link to ensure visual continuity. The size of a node's label reflects the frequency of
 1264 sequences containing the AoI at that position; by construction, the frequency at a node is always greater
 1265 than or equal to the sum of its children. Word trees may be either *left-rooted* or *right-rooted*, enabling
 1266 analysts to examine which AoIs tend to precede or follow a given region of interest.

1267 Word trees have been integrated into several visual analysis tools, including eSeeTrack (Tsang et al.
 1268 (2010)) and EyeC (Ristovski et al. (2013)), often in combination with other visualization techniques. For
 1269 example, eSeeTrack merges word trees with AoI clouds and suffix-tree-based representations to support
 1270 exploratory analysis of AoI sequences. Building on this concept, AoI transition trees (Kurzhals and
 1271 Weiskopf (2015)) have been proposed to visualize gaze patterns using thumbnail images to represent AoIs,
 1272 with thumbnail size encoding frequency. While this compact representation improves visual efficiency, it

1273 lacks one of the key advantages of word trees: explicit textual labeling, which allows analysts to directly
1274 interpret the semantic content of gaze paths.

1275 However, these approaches are generally limited to relatively short sequences. For long or highly variable
1276 sequences, inter-participant differences become too pronounced, effectively fragmenting viewers into
1277 distinct groups. To address this limitation, Kurzhals and Weiskopf (2015) proposed extending a single
1278 AoI transition tree into a *sequence of AoI transition trees*. This approach is particularly well suited to
1279 dynamic stimuli composed of successive scenes or semantically distinct segments. By exploiting natural
1280 temporal or semantic boundaries, a *divide-and-conquer* strategy can be applied to partition gaze data into
1281 coherent sections. Transition trees are then constructed for each segment, and corresponding AoIs across
1282 consecutive trees may be linked, yielding a sequence of smaller, interpretable transition trees rather than
1283 a single, visually overwhelming structure. As noted by Kurzhals and Weiskopf (2015), many dynamic
1284 stimuli can be naturally decomposed into semantically coherent units—such as task phases—allowing this
1285 approach to generalize across a wide range of experimental paradigms.

7 DISCUSSION

1286 The study of areas of interest and gaze dynamics constitutes a cornerstone of eye-tracking research and,
1287 more broadly, of the investigation of human attention, perception, and behavior. By combining cognitive
1288 theory, computational modeling, and experimental observation, this interdisciplinary field has progressively
1289 established itself as a key methodological framework for understanding how visual information is sampled,
1290 structured, and exploited by observers. Recent advances in eye-tracking technology — including remote,
1291 mobile, and wearable devices — have dramatically increased both the ecological validity and the volume
1292 of gaze data that can be collected. These developments have enabled the analysis of gaze behavior across
1293 a wide range of contexts, from highly controlled laboratory experiments to naturalistic and real-world
1294 environments.

1295 Despite these technological advances, the interpretation of gaze data remains intrinsically challenging.
1296 Visual trajectories are high-dimensional, noisy, and highly variable across individuals, tasks, and stimuli.
1297 Extracting meaningful visual strategies from such data therefore requires a careful balance between
1298 abstraction and fidelity to the original signal. As discussed throughout this review series (Laborde et al.
1299 (2024a,b,c)), progress in this domain depends not only on improvements in hardware precision, but also on
1300 the development of robust methodological frameworks capable of capturing both individual variability and
1301 group-level regularities.

1302 A central theme emerging from this work is the role of abstraction in gaze analysis. Areas of interest, AoI
1303 sequences, transition models, and representative scanpaths all rely on transforming raw gaze recordings
1304 into symbolic or structured representations. While such abstraction is indispensable for quantitative
1305 analysis, it inevitably entails a loss of information, particularly with respect to fine-grained spatial detail,
1306 temporal micro-dynamics, and idiosyncratic viewing behaviors. The challenge, therefore, is not to eliminate
1307 abstraction, but to control it — ensuring that the chosen level of representation remains appropriate to the
1308 research question at hand. In particular, once areas of interest are defined, they constitute the symbolic
1309 alphabet from which AoI sequences are constructed. This makes the AoI definition stage a pivotal upstream
1310 decision, as it conditions the statistical and structural properties of all subsequent sequence-based analyses.

1311 Within this context, visualization techniques play a crucial mediating role. Spatio-temporal visualizations,
1312 transition-based diagrams, and sequence-oriented representations provide an interpretable interface between
1313 raw gaze data and abstract computational models. These tools are particularly valuable for exploratory

1314 analysis, hypothesis generation, and qualitative validation, allowing researchers to visually inspect temporal
1315 structures, recurrent patterns, or anomalous behaviors before formalizing them quantitatively. However, as
1316 emphasized in this review, visualization methods are predominantly qualitative and descriptive. While they
1317 offer powerful insights into gaze dynamics, they do not, on their own, provide the formal rigor required for
1318 systematic comparison, statistical inference, or model-based prediction.

1319 Conversely, a wide range of quantitative approaches — including Markov-based models, entropy
1320 measures, pattern-mining algorithms, and consensus sequence methods — enable the formal
1321 characterization of gaze behavior. Many of these techniques originate from domains such as bioinformatics,
1322 information theory, or data mining, and have been adapted to the specific constraints of eye-tracking data.
1323 These methods make it possible to quantify visual strategies, compare observer groups, and relate gaze
1324 behavior to task demands, expertise, or cognitive load. Rather than opposing qualitative and quantitative
1325 paradigms, the results of this review highlight the necessity of their integration. Visualization supports
1326 interpretability and validation, while quantitative modeling provides formalization, generalization, and
1327 reproducibility. Effective gaze analysis workflows therefore rely on iterative interactions between these two
1328 perspectives.

1329 Another key issue concerns the scalability and generality of existing methods. Many algorithms perform
1330 well on small or moderately sized datasets, or under assumptions of limited inter-individual variability.
1331 However, as datasets grow larger and experimental designs become more complex — particularly in
1332 naturalistic or dynamic settings — the limitations of certain approaches become apparent. Some methods
1333 struggle with computational complexity, others with sensitivity to parameter choices, and others with
1334 their ability to accommodate heterogeneous visual strategies without excessive information loss. These
1335 limitations underscore the need for adaptive, data-driven approaches capable of balancing robustness and
1336 interpretability.

1337 The increasing methodological sophistication of gaze analysis also raises important challenges in terms
1338 of expertise and collaboration. Quantitative methods for AoI sequence analysis often require advanced
1339 knowledge in applied mathematics, statistics, or algorithm design, while neurophysiological, clinical,
1340 and ergonomic expertise remains essential for grounding computational findings in meaningful cognitive
1341 interpretations. As a result, the analysis of gaze dynamics — encompassing raw gaze data, scanpaths, and
1342 AoI-based representations — increasingly demands genuinely multidisciplinary research efforts, as well as
1343 shared conceptual frameworks and methodological vocabularies.

1344 Finally, reproducibility and methodological transparency remain critical challenges for the field. Beyond
1345 issues of implementation and reporting, a more fundamental difficulty lies in the inherently ill-posed nature
1346 of several core steps in AoI-based gaze analysis. Different, yet equally plausible, modeling assumptions for
1347 AoI definition, sequence abstraction, or transition estimation can lead to markedly different representations
1348 of visual behavior. As a result, downstream analyses—such as transition modeling, pattern mining, or
1349 consensus sequence extraction—may vary substantially depending on upstream methodological choices.

1350 In practice, the large volume and complexity of gaze data necessitate standardized preprocessing pipelines
1351 to ensure data quality and comparability across studies. At the same time, many algorithms used for
1352 AoI definition and sequence analysis are highly parameter-dependent, and these parameter choices
1353 are not always fully reported or systematically justified. Moreover, the absence of openly accessible
1354 implementations for some widely used methods further complicates replication, benchmarking, and
1355 meaningful methodological comparison.

1356 Addressing these issues is essential for consolidating gaze research into a cumulative and reproducible
1357 body of knowledge. Clearer methodological reporting, sensitivity analyses with respect to parameter
1358 choices, and systematic comparative evaluations are therefore indispensable for strengthening the reliability
1359 and interpretability of AoI-based gaze analyses.

1360 Looking ahead, several research directions emerge as particularly important for advancing the analysis
1361 of gaze dynamics. First, the definition and tracking of areas of interest in dynamic and interactive
1362 stimuli remains an open challenge: spatially similar fixations may correspond to temporally distinct
1363 or semantically different visual elements, limiting the validity of static AoI representations. Second,
1364 hybrid methodological pipelines that combine data-driven AoI inference, explicit temporal modeling,
1365 and interpretable visualization appear especially promising for balancing robustness, flexibility, and
1366 cognitive plausibility. Such approaches may help reconcile the need for abstraction with the preservation of
1367 meaningful temporal structure.

1368 More broadly, future progress will depend on the adoption of shared evaluation protocols, benchmark
1369 datasets, and reporting standards that make methodological choices explicit and results comparable
1370 across studies, tasks, and populations. By clarifying the assumptions underlying AoI definition, sequence
1371 abstraction, and model selection, the field can move toward more principled and transparent analyses.
1372 Ultimately, strengthening these foundations will enable gaze research to better integrate qualitative insight
1373 and quantitative rigor, and to more reliably link observed visual behavior to underlying cognitive and
1374 perceptual processes.

CONFLICT OF INTEREST STATEMENT

1375 Author QL was employed by company SNCF. Author AR was employed by company Thales AVS France.
1376 The remaining authors declare that the research was conducted in the absence of any commercial or
1377 financial relationships that could be construed as a potential conflict of interest.

AUTHOR CONTRIBUTIONS

1378 QL: Formal Analysis, Methodology, Writing – original draft, Writing – review & editing. AR: Formal
1379 Analysis, Writing – original draft, Writing – review & editing. AA: Validation, Writing – review & editing.
1380 NV: Supervision, Methodology, Validation, Writing – review & editing. IB: Supervision, Methodology,
1381 Validation, Writing – review & editing. LO: Supervision, Methodology, Validation, Writing – review &
1382 editing.

ACKNOWLEDGMENTS

1383 Part of this work has been founded by the Industrial Data Analytics And Machine Learning chairs of ENS
1384 Paris-Saclay.

REFERENCES

- 1385 Achanta, R., Hemami, S., Estrada, F., and Susstrunk, S. (2009). Frequency-tuned salient region detection.
1386 In *2009 IEEE conference on computer vision and pattern recognition* (IEEE), 1597–1604
- 1387 Agrawal, R., Imieliński, T., and Swami, A. (1993). Mining association rules between sets of items in large
1388 databases. In *Proceedings of the 1993 ACM SIGMOD international conference on Management of data*.
1389 207–216
- 1390 Agrawal, R. and Srikant, R. (1995). Mining sequential patterns. In *Proceedings of the eleventh international
1391 conference on data engineering* (IEEE), 3–14
- 1392 Agrawal, R., Srikant, R., et al. (1994). Fast algorithms for mining association rules. In *Proc. 20th int. conf.
1393 very large data bases, VLDB* (Santiago, Chile), vol. 1215, 487–499
- 1394 Ahsan, Z. and Obaidullah, U. (2023). Is clustering novice programmers possible? investigating scanpath
1395 trend analysis in programming tasks. In *Proceedings of the 2023 Symposium on Eye Tracking Research
1396 and Applications*. 1–7
- 1397 Albanesi, M. G., Gatti, R., Porta, M., and Ravarelli, A. (2011). Towards semi-automatic usability analysis
1398 through eye tracking. In *Proceedings of the 12th International Conference on Computer Systems and
1399 Technologies*. 135–141
- 1400 Arbelaez, P., Maire, M., Fowlkes, C., and Malik, J. (2010). Contour detection and hierarchical image
1401 segmentation. *IEEE transactions on pattern analysis and machine intelligence* 33, 898–916
- 1402 Arora, N., Fung, G., and Tunuguntla, S. (2017). T-patterns in business. Available at SSRN 3066839
- 1403 Atweh, J. A., Hayek, J. A., and Riggs, S. L. (2023). Quantifying visual attention of teams during
1404 workload transitions using aoi-based cross-recurrence metrics. In *Proceedings of the Human
1405 Factors and Ergonomics Society Annual Meeting* (SAGE Publications Sage CA: Los Angeles, CA),
1406 21695067231193683
- 1407 Ayres, J., Flannick, J., Gehrke, J., and Yiu, T. (2002). Sequential pattern mining using a bitmap
1408 representation. In *Proceedings of the eighth ACM SIGKDD international conference on Knowledge
1409 discovery and data mining*. 429–435
- 1410 Bakardzhiev, H., van der Burgt, M., Martins, E., van den Dool, B., Jansen, C., van Scheppingen, D., et al.
1411 (2021). A web-based eye tracking data visualization tool. In *Pattern Recognition. ICPR International
1412 Workshops and Challenges: Virtual Event, January 10–15, 2021, Proceedings, Part III* (Springer),
1413 405–419
- 1414 Barz, M., Bhatti, O. S., Alam, H. M. T., Nguyen, D. M. H., and Sonntag, D. (2023). Interactive fixation-
1415 to-aoi mapping for mobile eye tracking data based on few-shot image classification. In *Companion
1416 Proceedings of the 28th International Conference on Intelligent User Interfaces*. 175–178
- 1417 Bednarik, R., Myller, N., Sutinen, E., and Tukiainen, M. (2005). Applying eye-movement tracking to
1418 program visualization. *Proceedings of the 2005 IEEE Symposium on Visual Languages and Human-
1419 Centric Computing*, 302–304
- 1420 Bergroth, L., Hakonen, H., and Raita, T. (2000). A survey of longest common subsequence algorithms. In
1421 *Proceedings Seventh International Symposium on String Processing and Information Retrieval. SPIRE
1422 2000* (IEEE), 39–48
- 1423 Bianco, S., Gasparini, F., and Schettini, R. (2015). Color coding for data visualization. In *Encyclopedia of
1424 Information Science and Technology, Third Edition* (IGI Global). 1682–1691
- 1425 Bilmes, J. A. et al. (1998). A gentle tutorial of the em algorithm and its application to parameter estimation
1426 for gaussian mixture and hidden markov models. *International computer science institute* 4, 126
- 1427 Bishop, C. (2006). Pattern recognition and machine learning. *Springer google schola* 2, 35–42

- 1428 Blascheck, T., Kurzhals, K., Raschke, M., Burch, M., Weiskopf, D., and Ertl, T. (2014). State-of-the-art of
1429 visualization for eye tracking data. In *Eurovis (stars)*. 29
- 1430 Blascheck, T., Kurzhals, K., Raschke, M., Burch, M., Weiskopf, D., and Ertl, T. (2017). Visualization
1431 of eye tracking data: A taxonomy and survey. In *Computer Graphics Forum* (Wiley Online Library),
1432 vol. 36, 260–284
- 1433 Blascheck, T., Kurzhals, K., Raschke, M., Strohmaier, S., Weiskopf, D., and Ertl, T. (2016). Aoi hierarchies
1434 for visual exploration of fixation sequences. In *Proceedings of the Ninth Biennial ACM Symposium on*
1435 *Eye Tracking Research & Applications*. 111–118
- 1436 Blascheck, T., Raschke, M., and Ertl, T. (2013). Circular heat map transition diagram. In *Proceedings of*
1437 *the 2013 Conference on Eye Tracking South Africa*. 58–61
- 1438 Boisvert, J. F. and Bruce, N. D. (2016). Predicting task from eye movements: On the importance of spatial
1439 distribution, dynamics, and image features. *Neurocomputing* 207, 653–668
- 1440 Burch, M., Kull, A., and Weiskopf, D. (2013). Aoi rivers for visualizing dynamic eye gaze frequencies. In
1441 *Computer Graphics Forum* (Wiley Online Library), vol. 32, 281–290
- 1442 Burch, M., Kumar, A., and Mueller, K. (2018). The hierarchical flow of eye movements. In *Proceedings of*
1443 *the 3rd Workshop on Eye Tracking and Visualization*. 1–5
- 1444 Burch, M., Raschke, M., and Weiskopf, D. (2010). Indented pixel tree plots. In *Advances in Visual*
1445 *Computing: 6th International Symposium, ISVC 2010, Las Vegas, NV, USA, November 29–December 1,*
1446 *2010. Proceedings, Part I 6* (Springer), 338–349
- 1447 Burch, M., Wallner, G., Broeks, N., Piree, L., Boonstra, N., Vlaswinkel, P., et al. (2021). The power of
1448 linked eye movement data visualizations. In *ACM symposium on eye tracking research and applications*.
1449 1–11
- 1450 Burmester, M. and Mast, M. (2010). Repeated web page visits and the scanpath theory: A recurrent pattern
1451 detection approach. *Journal of Eye Movement Research* 3
- 1452 Castner, N., Geßler, L., Geisler, D., Hüttig, F., and Kasneci, E. (2020a). Towards expert gaze modeling and
1453 recognition of a user's attention in realtime. *Procedia Computer Science* 176
- 1454 Castner, N., Kuebler, T. C., Scheiter, K., Richter, J., Eder, T., Hüttig, F., et al. (2020b). Deep semantic gaze
1455 embedding and scanpath comparison for expertise classification during opt viewing. In *ACM Symposium*
1456 *on Eye Tracking Research and Applications*. 1–10
- 1457 Chen, X. and Chen, Z. (2017). Exploring visual attention using random walks based eye tracking protocols.
1458 *Journal of Visual Communication and Image Representation* 45, 147–155
- 1459 Chuk, T., Chan, A. B., and Hsiao, J. H. (2014). Understanding eye movements in face recognition using
1460 hidden markov models. *Journal of vision* 14, 8–8
- 1461 Chuk, T., Chan, A. B., and Hsiao, J. H. (2017). Is having similar eye movement patterns during face
1462 learning and recognition beneficial for recognition performance? evidence from hidden markov modeling.
1463 *Vision research* 141, 204–216
- 1464 Church, K. W. and Helfman, J. I. (1993). Dotplot: A program for exploring self-similarity in millions of
1465 lines of text and code. *Journal of Computational and Graphical Statistics* 2, 153–174
- 1466 Claus, M., Hermens, F., and Bromuri, S. (2023). A user study of visualisations of spatio-temporal eye
1467 tracking data. *arXiv preprint arXiv:2309.15731*
- 1468 Connor, M. C., Glass, B. H., Finkenstaedt-Quinn, S. A., and Shultz, G. V. (2020). Developing expertise in
1469 ^1H nmr spectral interpretation. *The Journal of Organic Chemistry* 86, 1385–1395
- 1470 Coutrot, A., Hsiao, J. H., and Chan, A. B. (2018). Scanpath modeling and classification with hidden
1471 markov models. *Behavior research methods* 50, 362–379

- 1472 Coviello, E., Chan, A. B., and Lanckriet, G. R. (2014). Clustering hidden markov models with variational
1473 hem. *The Journal of Machine Learning Research* 15, 697–747
- 1474 Coviello, E., Lanckriet, G., and Chan, A. (2012). The variational hierarchical em algorithm for clustering
1475 hidden markov models. *Advances in neural information processing systems* 25
- 1476 Crowe, E. C. and Narayanan, N. H. (2000). Comparing interfaces based on what users watch and do. In
1477 *Proceedings of the 2000 symposium on Eye tracking research & applications*. 29–36
- 1478 Dayan, P. (1993). Improving generalization for temporal difference learning: The successor representation.
1479 *Neural computation* 5, 613–624
- 1480 Drusch, G. and Bastien, J. C. (2012). Analyzing visual scanpaths on the web using the mean shift procedure
1481 and t-pattern detection: a bottom-up approach. In *Proceedings of the 2012 conference on ergonomie et*
1482 *interaction homme-machine*. 181–184
- 1483 Duchowski, A. T., Driver, J., Jolaoso, S., Tan, W., Ramey, B. N., and Robbins, A. (2010). Scanpath
1484 comparison revisited. In *Proceedings of the 2010 symposium on eye-tracking research & applications*.
1485 219–226
- 1486 Elbattah, M., Carette, R., Cilia, F., Guérin, J.-L., and Dequen, G. (2023). Applications of machine learning
1487 methods to assist the diagnosis of autism spectrum disorder. In *Neural Engineering Techniques for*
1488 *Autism Spectrum Disorder, Volume 2* (Elsevier). 99–119
- 1489 Ellahi, W. (2022). *Measuring and comparing visual attention deployment: application to Quality of*
1490 *Experience assessment in the context of hyper-realistic content*. Ph.D. thesis, Nantes Université
- 1491 Eraslan, S., Yesilada, Y., and Harper, S. (2014). Identifying patterns in eyetracking scanpaths in terms
1492 of visual elements of web pages. In *Web Engineering: 14th International Conference, ICWE 2014,*
1493 *Toulouse, France, July 1-4, 2014. Proceedings 14* (Springer), 163–180
- 1494 Eraslan, S., Yesilada, Y., and Harper, S. (2016). Scanpath trend analysis on web pages: Clustering eye
1495 tracking scanpaths. *ACM Transactions on the Web (TWEB)* 10, 1–35
- 1496 Eraslan, S., Yesilada, Y., and Harper, S. (2017). Engineering web-based interactive systems: trend
1497 analysis in eye tracking scanpaths with a tolerance. In *Proceedings of the ACM SIGCHI symposium on*
1498 *engineering interactive computing systems*. 3–8
- 1499 Eraslan, S., Yesilada, Y., Yaneva, V., and Harper, S. (2020). Autism detection based on eye movement
1500 sequences on the web: a scanpath trend analysis approach. In *Proceedings of the 17th International Web*
1501 *for All Conference*. 1–10
- 1502 Ester, M., Kriegel, H.-P., Sander, J., Xu, X., et al. (1996). A density-based algorithm for discovering
1503 clusters in large spatial databases with noise. In *kdd*. vol. 96, 226–231
- 1504 Fischer, P. and Peinsipp-Byma, E. (2007). Eye tracking for objective usability evaluation. In *European*
1505 *Conference on Eye Movements (ECEM)*. ECEM
- 1506 Fitts, P. M., Jones, R. E., and Milton, J. L. (2005). Eye movements of aircraft pilots during instrument-
1507 landing approaches. *Ergonomics: Major Writings*
- 1508 Frey, B. J. and Dueck, D. (2007). Clustering by passing messages between data points. *science* 315,
1509 972–976
- 1510 Fuhl, W., Kübler, T., Sippel, K., Rosenstiel, W., and Kasneci, E. (2015). Arbitrarily shaped areas of interest
1511 based on gaze density gradient. In *European Conference on Eye Movements, ECEM*. vol. 8, 9
- 1512 Fuhl, W., Kübler, T. C., Santini, T., and Kasneci, E. (2018a). Automatic generation of saliency-based areas
1513 of interest for the visualization and analysis of eye-tracking data. In *VMV*. 47–54
- 1514 Fuhl, W., Kuebler, T. C., Brinkmann, H., Rosenberg, R., Rosenstiel, W., and Kasneci, E. (2018b). Region
1515 of interest generation algorithms for eye tracking data. In *Proceedings of the 3rd Workshop on Eye*
1516 *Tracking and Visualization (ETVIS'18)* (ACM)

- 1517 Fukunaga, K. and Hostetler, L. (1975). The estimation of the gradient of a density function, with
1518 applications in pattern recognition. *IEEE Transactions on information theory* 21, 32–40
- 1519 Geisler, D., Castner, N., Kasneci, G., and Kasneci, E. (2020). A minhash approach for fast scanpath
1520 classification. In *ACM Symposium on Eye Tracking Research and Applications*. 1–9
- 1521 Gibbs, A. J. and McIntyre, G. A. (1970). The diagram, a method for comparing sequences: Its use with
1522 amino acid and nucleotide sequences. *European journal of biochemistry* 16, 1–11
- 1523 Goldberg, J. and Helfman, J. (2009). Pattern analysis in eye tracking data: Dotplots revisited. *Proceedings
1524 of the CHI 2009*
- 1525 Goldberg, J. H. and Helfman, J. I. (2010). Scanpath clustering and aggregation. In *Proceedings of the 2010
1526 symposium on eye-tracking research & applications*. 227–234
- 1527 Goldberg, J. H. and Kotval, X. P. (1999). Computer interface evaluation using eye movements: methods
1528 and constructs. *International journal of industrial ergonomics* 24, 631–645
- 1529 Guo, C., Ma, Q., and Zhang, L. (2008). Spatio-temporal saliency detection using phase spectrum of
1530 quaternion fourier transform. In *2008 IEEE conference on computer vision and pattern recognition
1531 (IEEE)*, 1–8
- 1532 Haji-Abolhassani, A. and Clark, J. J. (2013). A computational model for task inference in visual search.
1533 *Journal of vision* 13, 29–29
- 1534 Haji-Abolhassani, A. and Clark, J. J. (2014). An inverse yarbus process: Predicting observers' task from
1535 eye movement patterns. *Vision research* 103, 127–142
- 1536 Hao, Q., Ma, L., Sbert, M., Feixas, M., and Zhang, J. (2020). Gaze information channel in van gogh's
1537 paintings. *Entropy* 22, 540
- 1538 Hao, Q., Sbert, M., and Ma, L. (2019). Gaze information channel in cognitive comprehension of poster
1539 reading. *Entropy* 21, 444
- 1540 Hastie, T., Tibshirani, R., Friedman, J. H., and Friedman, J. H. (2009). *The elements of statistical learning:
1541 data mining, inference, and prediction*, vol. 2 (Springer)
- 1542 Hayes, T. R., Petrov, A. A., and Sederberg, P. B. (2011). A novel method for analyzing sequential eye
1543 movements reveals strategic influence on raven's advanced progressive matrices. *Journal of Vision* 11,
1544 10–10
- 1545 Hejmady, P. and Narayanan, N. H. (2012). Visual attention patterns during program debugging with an ide.
1546 In *proceedings of the symposium on eye tracking research and applications*. 197–200
- 1547 Hellinger, E. (1909). Neue begründung der theorie quadratischer formen von unendlichvielen
1548 veränderlichen. *Journal für die reine und angewandte Mathematik* 1909, 210–271
- 1549 Holmqvist, K., Holsanova, J., Barthelson, M., and Lundqvist, D. (2003). Reading or scanning? a study of
1550 newspaper and net paper reading. In *The Mind's Eye* (Elsevier). 657–670
- 1551 Holmqvist, K., Nystrom, M., Andersson, R., Dewhurst, R., Jarodzka, H., and Van de Weijer, J. (2011). Eye
1552 tracking: A comprehensive guide to methods and measures. *OUP Oxford*
- 1553 Hooge, I. and Camps, G. (2013). Scan path entropy and arrow plots: Capturing scanning behavior of
1554 multiple observers. *Frontiers in psychology* 4, 996
- 1555 Hou, X. and Zhang, L. (2007). Saliency detection: A spectral residual approach. In *2007 IEEE Conference
1556 on computer vision and pattern recognition* (Ieee), 1–8
- 1557 Hsiao, J. H., Lan, H., Zheng, Y., and Chan, A. B. (2021). Eye movement analysis with hidden markov
1558 models (emhmm) with co-clustering. *Behavior Research Methods* 53, 2473–2486
- 1559 Huang, H., Doebler, P., and Mertins, B. (2024). Short-time aois-based representative scanpath identification
1560 and scanpath aggregation. *Behavior Research Methods* , 1–16

- 1561 Huang, T.-H., Cheng, K.-Y., and Chuang, Y.-Y. (2009). A collaborative benchmark for region of interest
1562 detection algorithms. In *2009 IEEE Conference on Computer Vision and Pattern Recognition* (IEEE),
1563 296–303
- 1564 Huang, Y. and Zhang, L. (2004). Rapid and sensitive dot-matrix methods for genome analysis.
1565 *Bioinformatics* 20, 460–466
- 1566 Itoh, K., Hansen, J.-P., and Nielsen, F. (1998). Cognitive modelling of a ship navigator based on protocol
1567 and eye-movement analysis. *Le Travail Humain*, 99–127
- 1568 Itoh, K., Tanaka, H., and Seki, M. (2000). Eye-movement analysis of track monitoring patterns of night
1569 train operators: Effects of geographic knowledge and fatigue. In *Proceedings of the human factors and*
1570 *ergonomics society annual meeting* (SAGE Publications Sage CA: Los Angeles, CA), vol. 44, 360–363
- 1571 Itti, L., Koch, C., and Niebur, E. (1998). A model of saliency-based visual attention for rapid scene analysis.
1572 *IEEE Transactions on pattern analysis and machine intelligence* 20, 1254–1259
- 1573 Jayawardena, G. and Jayarathna, S. (2021). Automated filtering of eye movements using dynamic aoi in
1574 multiple granularity levels. *International Journal of Multimedia Data Engineering and Management*
1575 (*IJMDEM*) 12, 49–64
- 1576 Jraidi, I., Chaouachi, M., Ben Khedher, A., Lajoie, S. P., and Frasson, C. (2022). Understanding clinical
1577 reasoning through visual scanpath and brain activity analysis. *Computation* 10, 130
- 1578 Just, M. A. and Carpenter, P. A. (1980). A theory of reading: from eye fixations to comprehension.
1579 *Psychological review* 87, 329
- 1580 Kanan, C., Bseiso, D. N., Ray, N. A., Hsiao, J. H., and Cottrell, G. W. (2015). Humans have idiosyncratic
1581 and task-specific scanpaths for judging faces. *Vision research* 108, 67–76
- 1582 Kanan, C., Ray, N. A., Bseiso, D. N., Hsiao, J. H., and Cottrell, G. W. (2014). Predicting an observer's task
1583 using multi-fixation pattern analysis. In *Proceedings of the symposium on eye tracking research and*
1584 *applications*. 287–290
- 1585 Kaufman, L. and Rousseeuw, P. J. (2009). *Finding groups in data: an introduction to cluster analysis* (John
1586 Wiley & Sons)
- 1587 Kopácsi, L., Barz, M., Bhatti, O. S., and Sonntag, D. (2023). Imeta: An interactive mobile eye tracking
1588 annotation method for semi-automatic fixation-to-aoi mapping. In *Companion Proceedings of the 28th*
1589 *International Conference on Intelligent User Interfaces*. 33–36
- 1590 Kosel, C., Holzberger, D., and Seidel, T. (2021). Identifying expert and novice visual scanpath patterns
1591 and their relationship to assessing learning-relevant student characteristics. In *Frontiers in*
1592 *Education* (Frontiers Media SA), vol. 5, 612175
- 1593 Krejtz, I., Szarkowska, A., and Krejtz, K. (2013). The effects of shot changes on eye movements in
1594 subtitling
- 1595 Krejtz, K., Duchowski, A., Szmidt, T., Krejtz, I., González Perilli, F., Pires, A., et al. (2015). Gaze
1596 transition entropy. *ACM Transactions on Applied Perception (TAP)* 13, 1–20
- 1597 Krejtz, K., Szmidt, T., Duchowski, A. T., and Krejtz, I. (2014). Entropy-based statistical analysis of eye
1598 movement transitions. In *Proceedings of the Symposium on Eye Tracking Research and Applications*.
1599 159–166
- 1600 Kübler, T. C., Rothe, C., Schiefer, U., Rosenstiel, W., and Kasneci, E. (2017). Subsmatch 2.0: Scanpath
1601 comparison and classification based on subsequence frequencies. *Behavior research methods* 49,
1602 1048–1064
- 1603 Kurzhals, K., Burch, M., Blascheck, T., Andrienko, G., Andrienko, N., and Weiskopf, D. (2017). A task-
1604 based view on the visual analysis of eye-tracking data. In *Eye Tracking and Visualization: Foundations,*
1605 *Techniques, and Applications. ETVIS 2015 1* (Springer), 3–22

- 1606 Kurzhals, K., Hlawatsch, M., Heimerl, F., Burch, M., Ertl, T., and Weiskopf, D. (2015). Gaze stripes:
1607 Image-based visualization of eye tracking data. *IEEE transactions on visualization and computer
1608 graphics* 22, 1005–1014
- 1609 Kurzhals, K., Hlawatsch, M., Seeger, C., and Weiskopf, D. (2016). Visual analytics for mobile eye tracking.
1610 *IEEE transactions on visualization and computer graphics* 23, 301–310
- 1611 Kurzhals, K. and Weiskopf, D. (2013). Space-time visual analytics of eye-tracking data for dynamic stimuli.
1612 *IEEE Transactions on Visualization and Computer Graphics* 19, 2129–2138
- 1613 Kurzhals, K. and Weiskopf, D. (2015). Aoi transition trees. In *Graphics Interface*. 41–48
- 1614 Laborde, Q., Roques, A., Bargiotas, I., Armougum, A., Vayatis, N., and Oudre, L. (2024a). Vision part 1:
1615 Neurophysiology and experimental paradigms [manuscript submitted for publication]. *Université Paris
1616 Saclay, Université Paris Cité, ENS Paris Saclay, CNRS, SSA, INSERM, Centre Borelli, F-91190, France*
- 1617 Laborde, Q., Roques, A., Bargiotas, I., Armougum, A., Vayatis, N., and Oudre, L. (2024b). Vision part
1618 2: Oculomotor processing [manuscript submitted for publication]. *Université Paris Saclay, Université
1619 Paris Cité, ENS Paris Saclay, CNRS, SSA, INSERM, Centre Borelli, F-91190, France*
- 1620 Laborde, Q., Roques, A., Bargiotas, I., Armougum, A., Vayatis, N., and Oudre, L. (2024c). Vision part 3:
1621 Scanpaths and derived representations [manuscript submitted for publication]. *Université Paris Saclay,
1622 Université Paris Cité, ENS Paris Saclay, CNRS, SSA, INSERM, Centre Borelli, F-91190, France*
- 1623 Lagmay, E. A. D., Rodrigo, M. M. T., et al. (2022). Enhanced automatic areas of interest (aoi) bounding
1624 boxes estimation algorithm for dynamic eye-tracking stimuli. *APSIPA Transactions on Signal and
1625 Information Processing* 11
- 1626 Latimer, C. R. (1988). Eye-movement data: Cumulative fixation time and cluster analysis. *Behavior
1627 Research Methods, Instruments, & Computers* 20, 437–470
- 1628 Lempel, A. and Ziv, J. (1976). On the complexity of finite sequences. *IEEE Transactions on information
1629 theory* 22, 75–81
- 1630 Li, A. and Chen, Z. (2018). Representative scanpath identification for group viewing pattern analysis.
1631 *Journal of Eye Movement Research* 11
- 1632 Li, A., Zhang, Y., and Chen, Z. (2017). Scanpath mining of eye movement trajectories for visual attention
1633 analysis. In *2017 IEEE International Conference on Multimedia and Expo (ICME)* (IEEE), 535–540
- 1634 Lounis, C., Peysakhovich, V., and Causse, M. (2020). Complexity of dwell sequences: visual scanning
1635 pattern differences between novice and expert aircraft pilots. In *1st International Workshop on Eye-
1636 Tracking in Aviation*
- 1637 Lounis, C., Peysakhovich, V., and Causse, M. (2021). Visual scanning strategies in the cockpit are
1638 modulated by pilots' expertise: A flight simulator study. *PLoS one* 16, e0247061
- 1639 Ma, R. and Angryk, R. (2017). Distance and density clustering for time series data. In *2017 IEEE
1640 international conference on data mining workshops (ICDMW)* (IEEE), 25–32
- 1641 Ma, X., Liu, Y., Clariana, R., Gu, C., and Li, P. (2023). From eye movements to scanpath networks: A
1642 method for studying individual differences in expository text reading. *Behavior research methods* 55,
1643 730–750
- 1644 Mackworth, N. H. and Morandi, A. J. (1967). The gaze selects informative details within pictures.
1645 *Perception & psychophysics* 2, 547–552
- 1646 Magnusson, M. S. (2000). Discovering hidden time patterns in behavior: T-patterns and their detection.
1647 *Behavior research methods, instruments, & computers* 32, 93–110
- 1648 Maizel Jr, J. V. and Lenk, R. P. (1981). Enhanced graphic matrix analysis of nucleic acid and protein
1649 sequences. *Proceedings of the National Academy of Sciences* 78, 7665–7669

- 1650 Marchal, F., Castagnos, S., and Boyer, A. (2016). Tell me what you see, i will tell you what you remember.
1651 In *Proceedings of the 2016 Conference on User Modeling Adaptation and Personalization*. 293–294
- 1652 Mast, M. and Burmester, M. (2011). Exposing repetitive scanning in eye movement sequences with
1653 t-pattern detection. In *Proceedings IADIS International conference interfaces and human computer*
1654 *interaction (IHCI)*. 137–145
- 1655 McGrory, C. A. and Titterington, D. (2009). Variational bayesian analysis for hidden markov models.
1656 *Australian & New Zealand Journal of Statistics* 51, 227–244
- 1657 McGuire, M. P. and Chakraborty, J. (2016). Directional scan path characterization of eye tracking
1658 sequences: A multi-scale approach. In *2016 Future Technologies Conference (FTC)* (IEEE), 51–61
- 1659 McIntyre, N. A., Mainhard, M. T., and Klassen, R. M. (2017). Are you looking to teach? cultural, temporal
1660 and dynamic insights into expert teacher gaze. *Learning and Instruction* 49, 41–53
- 1661 Melsted, P. and Pritchard, J. K. (2011). Efficient counting of k-mers in dna sequences using a bloom filter.
1662 *BMC bioinformatics* 12, 1–7
- 1663 Meyer, C. (2000). Perron–frobenius theory of nonnegative matrices. *Matrix analysis and applied linear*
1664 *algebra*, SIAM
- 1665 Naqshbandi, K., Gedeon, T., and Abdulla, U. A. (2016). Automatic clustering of eye gaze data for machine
1666 learning. In *2016 IEEE International Conference on Systems, Man, and Cybernetics (SMC)* (IEEE),
1667 001239–001244
- 1668 Nguyen, A., Chandran, V., and Sridharan, S. (2006). Gaze tracking for region of interest coding in jpeg
1669 2000. *Signal Processing: Image Communication* 21, 359–377
- 1670 Obaidellah, U., Blascheck, T., Guarnera, D. T., and Maletic, J. (2020). A fine-grained assessment on novice
1671 programmers’ gaze patterns on pseudocode problems. In *ACM Symposium on Eye Tracking Research*
1672 *and Applications*. 1–5
- 1673 Opach, T., Golebiowska, I., and Fabrikant, S. I. (2014). How do people view multi-component animated
1674 maps? *The Cartographic Journal* 51, 330–342
- 1675 Petitjean, F., Ketterlin, A., and Gançarski, P. (2011). A global averaging method for dynamic time warping,
1676 with applications to clustering. *Pattern recognition* 44, 678–693
- 1677 Pillalamarri, R. S., Barnette, B. D., Birkmire, D., and Karsh, R. (1993). Cluster: A program for the
1678 identification of eye-fixation-cluster characteristics. *Behavior Research Methods, Instruments, &*
1679 *Computers* 25, 9–15
- 1680 Plummer, P., DeWolf, M., Bassok, M., Gordon, P. C., and Holyoak, K. J. (2017). Reasoning strategies with
1681 rational numbers revealed by eye tracking. *Attention, Perception, & Psychophysics* 79, 1426–1437
- 1682 Ponsoda, V., Scott, D., and Findlay, J. (1995). A probability vector and transition matrix analysis of eye
1683 movements during visual search. *Acta Psychologica* 88, 167–185
- 1684 Privitera, C. M. and Stark, L. W. (1998). Evaluating image processing algorithms that predict regions of
1685 interest. *Pattern Recognition Letters* 19, 1037–1043
- 1686 Privitera, C. M. and Stark, L. W. (2000). Algorithms for defining visual regions-of-interest: Comparison
1687 with eye fixations. *IEEE Transactions on pattern analysis and machine intelligence* 22, 970–982
- 1688 Qazi, M., Tunuguntla, S., Lee, P., Kanchinadam, T., Fung, G., and Arora, N. (2019). Discovering temporal
1689 patterns from insurance interaction data. In *Proceedings of the AAAI Conference on Artificial Intelligence*.
1690 vol. 33, 9573–9580
- 1691 Räihä, K.-J., Aula, A., Majaranta, P., Rantala, H., and Koivunen, K. (2005). Static visualization of
1692 temporal eye-tracking data. In *Human-Computer Interaction-INTERACT 2005: IFIP TC13 International*
1693 *Conference, Rome, Italy, September 12-16, 2005. Proceedings* 10 (Springer), 946–949

- 1694 Raschke, M., Chen, X., and Ertl, T. (2012). Parallel scan-path visualization. In *Proceedings of the*
1695 *Symposium on Eye Tracking Research and Applications*. 165–168
- 1696 Reani, M., Peek, N., and Jay, C. (2018). An investigation of the effects of n-gram length in scanpath
1697 analysis for eye-tracking research. *Proceedings of the 2018 ACM Symposium on Eye Tracking Research*
1698 & Applications , 1–8
- 1699 Rees, D., Laramee, R. S., Brookes, P., and D'Cruze, T. (2020). Interaction techniques for chord diagrams.
1700 In *2020 24th International Conference Information Visualisation (IV)* (IEEE), 28–37
- 1701 Richardson, D. C. and Dale, R. (2005). Looking to understand: The coupling between speakers' and
1702 listeners' eye movements and its relationship to discourse comprehension. *Cognitive science* 29,
1703 1045–1060
- 1704 Riehmann, P., Hanfler, M., and Froehlich, B. (2005). Interactive sankey diagrams. In *IEEE Symposium on*
1705 *Information Visualization, 2005. INFOVIS 2005*. (IEEE), 233–240
- 1706 Ristovski, G., Hunter, M., Olk, B., and Linsen, L. (2013). Eyec: Coordinated views for interactive visual
1707 exploration of eye-tracking data. In *2013 17th International Conference on Information Visualisation*
1708 (IEEE), 239–248
- 1709 Rodriguez, A. and Laio, A. (2014). Clustering by fast search and find of density peaks. *science* 344,
1710 1492–1496
- 1711 Salah, A. A., Pauwels, E., Tavenard, R., and Gevers, T. (2010). T-patterns revisited: mining for temporal
1712 patterns in sensor data. *Sensors* 10, 7496–7513
- 1713 Santella, A. and DeCarlo, D. (2004). Robust clustering of eye movement recordings for quantification of
1714 visual interest. In *Proceedings of the 2004 symposium on Eye tracking research & applications*. 27–34
- 1715 Setubal, J. C., Meidanis, J., and Setubal-Meidanis (1997). *Introduction to computational molecular biology*.
1716 04; QH506, S4. (PWS Pub. Boston)
- 1717 Shannon, C. E. (1948). A mathematical theory of communication. *The Bell system technical journal* 27,
1718 379–423
- 1719 Shi, J. and Malik, J. (2000). Normalized cuts and image segmentation. *IEEE Transactions on pattern*
1720 *analysis and machine intelligence* 22, 888–905
- 1721 Smith, T. F., Waterman, M. S., et al. (1981). Identification of common molecular subsequences. *Journal of*
1722 *molecular biology* 147, 195–197
- 1723 Špakov, O. and Miniotas, D. (2007). Application of clustering algorithms in eye gaze visualizations.
1724 *Information Technology and Control* 36
- 1725 Tablatin, C. L. and Rodrigo, M. M. (2018). Identifying common code reading patterns using scanpath
1726 trend analysis with a tolerance. In *Proceedings of the 26th International Conference for Computers in*
1727 *Education (ICCE 2018), Metro Manila, Philippines*
- 1728 Tang, H., Day, E., Kendhammer, L., Moore, J. N., Brown, S. A., and Pienta, N. J. (2016). Eye movement
1729 patterns in solving science ordering problems. *Journal of eye movement research* 9
- 1730 Tavenard, R., Salah, A. A., and Pauwels, E. J. (2008). Searching for temporal patterns in ami sensor data.
1731 In *Constructing Ambient Intelligence: AmI 2007 Workshops Darmstadt, Germany, November 7-10, 2007*
1732 *Revised Papers* (Springer), 53–62
- 1733 Tory, M., Atkins, M. S., Kirkpatrick, A. E., Nicolaou, M., and Yang, G.-Z. (2005). Eyegaze analysis of
1734 displays with combined 2d and 3d views. In *VIS 05. IEEE Visualization, 2005*. (IEEE), 519–526
- 1735 Trajkovska, K., Kljun, M., and Pucihar, K. Č. (2024). Gaze2aoi: Open source deep-learning based system
1736 for automatic area of interest annotation with eye tracking data. *arXiv preprint arXiv:2411.13346*
- 1737 Tsang, H. Y., Tory, M., and Swindells, C. (2010). eseetrack—visualizing sequential fixation patterns. *IEEE*
1738 *Transactions on Visualization and Computer Graphics* 16, 953–962

- 1739 Van Erven, T. and Harremos, P. (2014). Rényi divergence and kullback-leibler divergence. *IEEE
1740 Transactions on Information Theory* 60, 3797–3820
- 1741 Vandeberg, L., Bouwmeester, S., Bocanegra, B. R., and Zwaan, R. A. (2013). Detecting cognitive
1742 interactions through eye movement transitions. *Journal of Memory and Language* 69, 445–460
- 1743 Vassallo, S. and Douglas, J. (2021). Visual scanpath training to emotional faces following severe traumatic
1744 brain injury: A single case design. *Journal of Eye Movement Research* 14
- 1745 von der Malsburg, T., Kliegl, R., and Vasishth, S. (2015). Determinants of scanpath regularity in reading.
1746 *Cognitive science* 39, 1675–1703
- 1747 Von Landesberger, T., Kuijper, A., Schreck, T., Kohlhammer, J., van Wijk, J. J., Fekete, J.-D., et al. (2011).
1748 Visual analysis of large graphs: state-of-the-art and future research challenges. In *Computer graphics
1749 forum* (Wiley Online Library), vol. 30, 1719–1749
- 1750 Wagemans, J., Feldman, J., Gepshtain, S., Kimchi, R., Pomerantz, J. R., Van der Helm, P. A., et al.
1751 (2012). A century of gestalt psychology in visual perception: II. conceptual and theoretical foundations.
1752 *Psychological bulletin* 138, 1218
- 1753 Wang, F. S., Gianduzzo, C., Meboldt, M., and Lohmeyer, Q. (2022). An algorithmic approach to determine
1754 expertise development using object-related gaze pattern sequences. *Behavior Research Methods* 54,
1755 493–507
- 1756 Wang, Y., Chen, X., and Chen, Z. (2016). Towards region-of-attention analysis in eye tracking protocols.
1757 *Electronic Imaging* 2016, 1–6
- 1758 Wang, Z. (2021). Eye movement data analysis and visualization. In *Eye-Tracking with Python and Pylink*
1759 (Springer). 197–224
- 1760 Wattenberg, M. and Viégas, F. B. (2008). The word tree, an interactive visual concordance. *IEEE
1761 transactions on visualization and computer graphics* 14, 1221–1228
- 1762 Weibel, N., Fouse, A., Emmenegger, C., Kimmich, S., and Hutchins, E. (2012). Let's look at the cockpit:
1763 exploring mobile eye-tracking for observational research on the flight deck. In *Proceedings of the
1764 symposium on eye tracking research and applications*. 107–114
- 1765 West, J. M., Haake, A. R., Rozanski, E. P., and Karn, K. S. (2006). eyepatterns: software for identifying
1766 patterns and similarities across fixation sequences. In *Proceedings of the 2006 symposium on Eye
1767 tracking research & applications*. 149–154
- 1768 Yang, C.-K. and Wacharamanotham, C. (2018). Alpscarf: Augmenting scarf plots for exploring temporal
1769 gaze patterns. In *Extended abstracts of the 2018 CHI conference on human factors in computing systems*.
1770 1–6